REPORT DOCUMENTATION PAGE

Form Approved
OMB No. 0704-0188

1. REPORT DATE *(DD-MM-YYYY)*	**2. REPORT TYPE**	**3. DATES COVERED** *(From - To)*
July 2013	Viewgraph	July 2013- August 2013

4. TITLE AND SUBTITLE
Mixing in shear coaxial jets (Briefing Charts)

5a. CONTRACT NUMBER
In-House

5b. GRANT NUMBER

5c. PROGRAM ELEMENT NUMBER

6. AUTHOR(S)
Ivett Leyva

5d. PROJECT NUMBER

5e. TASK NUMBER

5f. WORK UNIT NUMBER
Q0YA

7. PERFORMING ORGANIZATION NAME(S) AND ADDRESS(ES)

Air Force Research Laboratory (AFMC)
AFRL/RQRC
10 E. Saturn Blvd
Edwards AFB CA 93524-7680

8. PERFORMING ORGANIZATION REPORT NO.

9. SPONSORING / MONITORING AGENCY NAME(S) AND ADDRESS(ES)
Air Force Research Laboratory (AFMC)
AFRL/RQR
5 Pollux Drive
Edwards AFB CA 93524-7048

10. SPONSOR/MONITOR'S ACRONYM(S)

11. SPONSOR/MONITOR'S REPORT NUMBER(S)
AFRL-RQ-ED-VG-2013-184

12. DISTRIBUTION / AVAILABILITY STATEMENT
Distribution A: Approved for Public Release; Distribution Unlimited. PA#13399

13. SUPPLEMENTARY NOTES
Viewgraph for the Giving talk at Technical University of Munich, Munich, Germany, 2 August 2013.

14. ABSTRACT
N/A

15. SUBJECT TERMS

16. SECURITY CLASSIFICATION OF:			**17. LIMITATION OF ABSTRACT**	**18. NUMBER OF PAGES**	**19a. NAME OF RESPONSIBLE PERSON**
a. REPORT	**b. ABSTRACT**	**c. THIS PAGE**			Douglas Talley
Unclassified	**Unclassified**	**Unclassified**	SAR	70	**19b. TELEPHONE NO** *(include area code)* 661-525-6174

Standard Form 298 (Rev. 8-98)
Prescribed by ANSI Std. 239.18

Mixing in Shear Coaxial Jets

RS-68 tested at AFRL Edwards, 2001

http://www.spacedaily.com/news/delta4-01f.html

Ivett A Leyva

Air Force Research Lab

Edwards AFB, CA, USA

Technical University of Munich

August 2013

Outline

- Description of shear coaxial jets
- Applications to rocket engines
- Survey of relevant previous works
  - Experiments
  - Numerical simulations
- AFRL's published research in the area
- Current challenges
- Conclusions

Anatomy of shear coaxial jets

Schematic

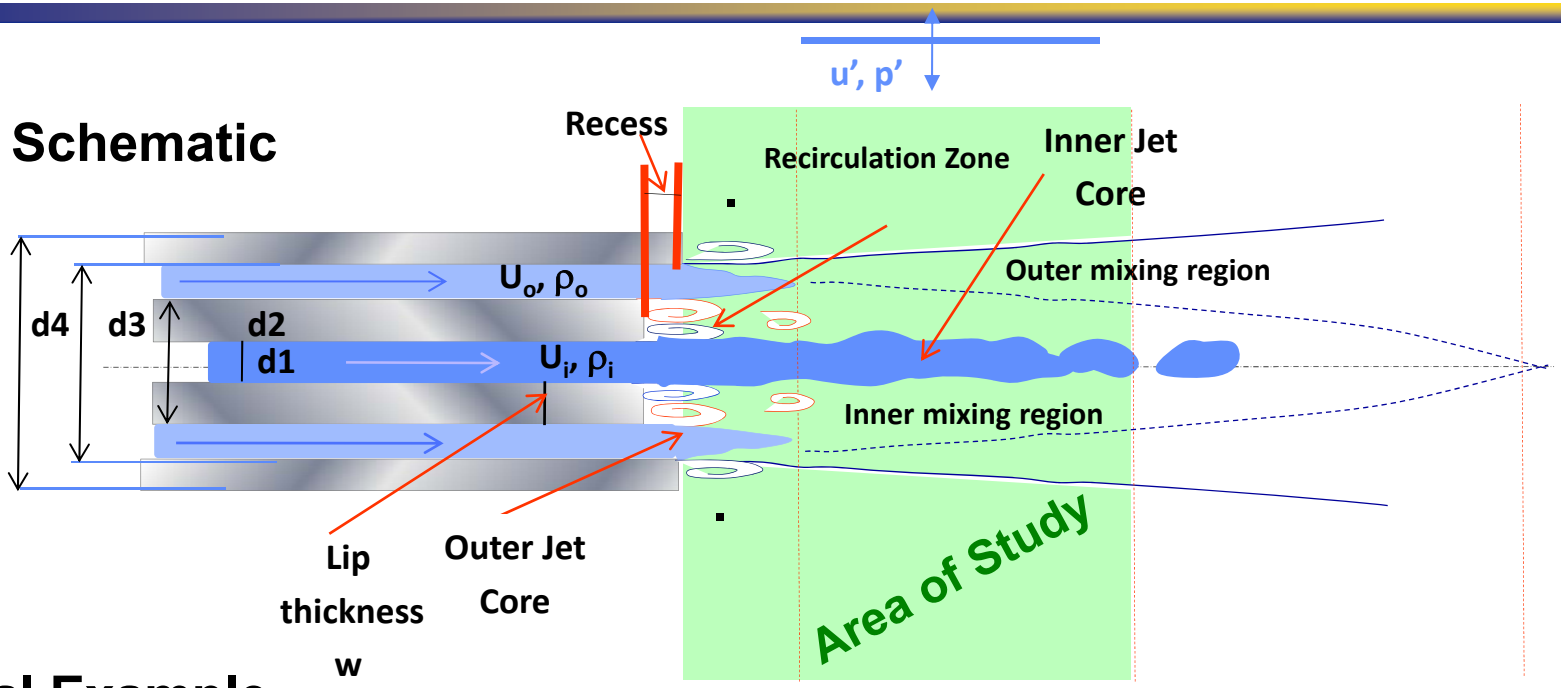

Real Example

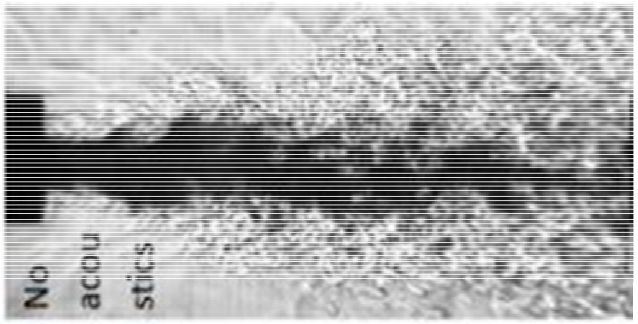

From J. I. Rodriguez. Acoustic Excitation of Liquid Fuel Droplets and Coaxial Jets. Ph.D. dissertation, UCLA, 2009.

Initial Merging Zone → Intermediate Merging Zone → Fully Merged Zone

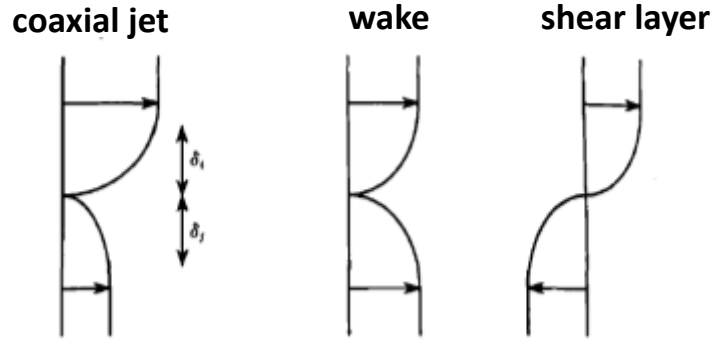

Dahm et al, JFM, Vol 241, 1992

Important flow and geometry parameters

1. **AR: Outer to inner jet Area Ratio**
2. **J: Outer to inner jet Momentum Flux Ratio,** $\rho_o U^2_o / \rho_i U^2_i$
3. **R: outer to inner jet velocity ratio,** U_o / U_i
4. **Re: Reynolds number for inner and outer jets,** $\rho_j U_j D_{hyd} / \mu_j$
5. **S: outer to inner jet density ratio, ,** ρ_o / ρ_i
6. *t/D*$_1$*:* **Inner jet lip thickness/inner diameter**
7. **We: Weber number if surface tension is present,** $\rho_g U_g 2 D_l / \sigma_l$
8. **Exit boundary layer profile – 3 relevant boundary layers**
9. **Thermodynamic states (2 phase, 1 phase)**
10. **Transverse Acoustic mode from chamber/siren, f=f(c, geometry**

    St=fD$_{ij}$/U$_{ij}$
11. **Acoustic modes for outer and inner jets**

    f~c/2L – 2 speeds of sound up and downstream
12. **Wake resulting from inner post thickness**

    St=fw/U$_{ch}$
13. **Shear layer instabilities**

    St$_\theta$=fθ/U$_{ch}$
14. **Jet preferred modes**

    St=fD$_{ij}$/U$_{ij}$

Some applications in rockets

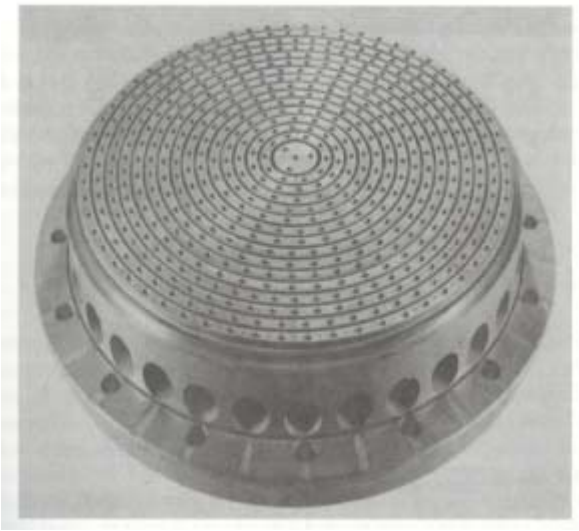

Space Shuttle Main Engine Injector face

Rocket Propulsion Elements (7th Edition), Sutton, G. P.; Biblarz, O. 2001

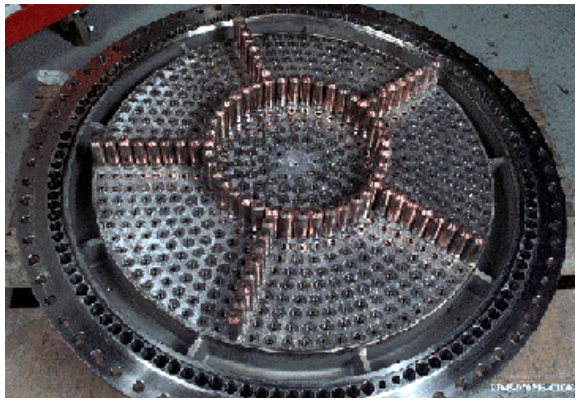

Prototype for RS-68

B. K. Wood, Propulsion for the 21st Century—RS-68, AIAA 2002-4324

Vulcain 2 from EADS ASTRIUM

http://cs.astrium.eads.net/sp/launcher-propulsion/rocket-engines/vulcain-2-rocket-engine.html

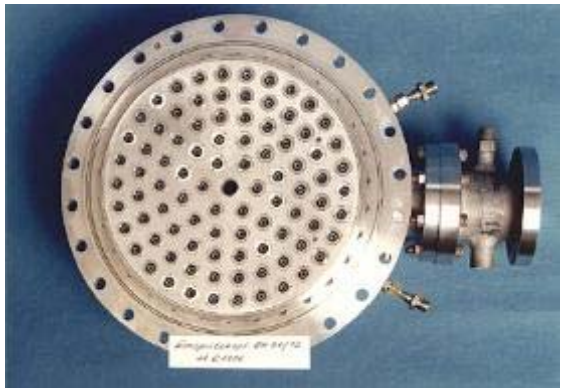

HM 7 from EADS ASTRIUM

http://cs.astrium.eads.net/sp/launcher-propulsion/rocket-engines/hm7b-rocket-engine.html

SSME view from nozzle exit

Injector Face with shear coaxial injectors

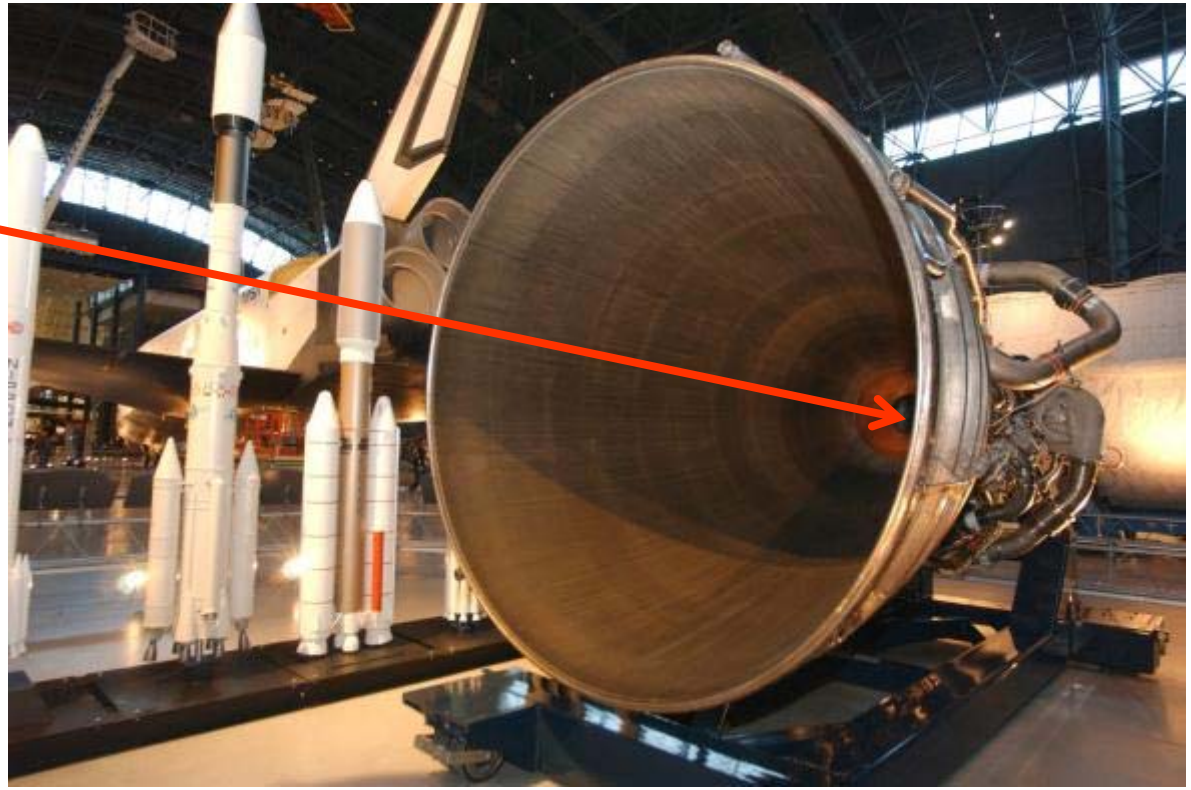

SSME

http://www.nasa.gov/images/content/68098main_nasm_ent_ssme_hires.jpg

What do we need to know about shear coaxial injectors?

- The mixing process between the inner and outer jets for different conditions:
  - If applicable, need to characterize droplet formation, droplet diameter distribution and vaporization
  - Modern rockets operate at supercritical pressures with respect to the propellants therefore also need to understand mixing and combustion beyond liquid and gas states
- An injector's own instability modes
- The interactions of transverse acoustics with injector's own instability modes and mixing processes
  - Need to understand differences in response to pressure and velocity nodes
- What non-dimensional numbers are most critical to define mixing and instability modes
- How injector geometry affects mixing and susceptibility to external disturbances

Consequence of incomplete knowledge – *Combustion Instabilities*

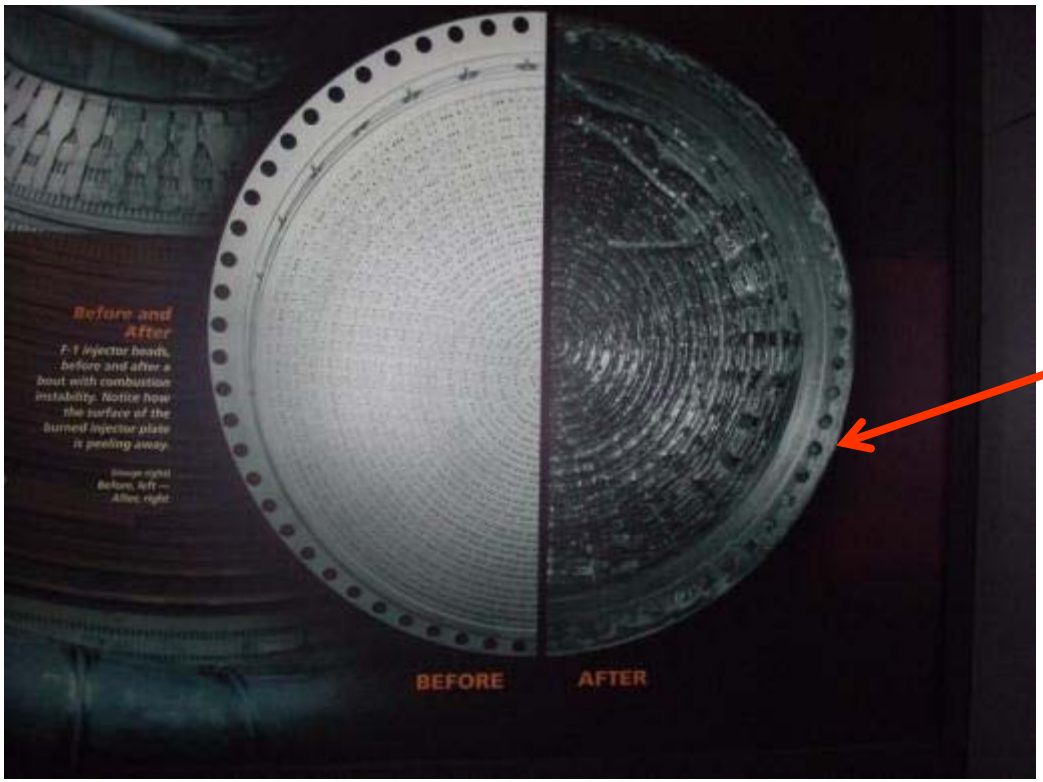

Injector head molten after a combustion instability event

Courtesy: U.S. Rocket and Space Center, Huntsville, AL

Combustion instability is an *unsustainable growth of pressure and heat transfer fluctuations in a rocket engine*

Irreparable damage can occur in <1s

Earlier contributors to the field 1/2

- Michalke, 1964
  - Linear stability theory for inviscid instability of a hyperbolic tangent velocity profile for free boundary layers
    - U(y)=0.5[1 + tanh(y)]
- Chigier and Beer, 1964
  - pioneering experimental work on uniform density air coaxial jets
  - detailed velocity and static pressure measurements of fully developed turbulent flow with t/D_1~1
  - After the two jets combine the behave as an equivalent single jet
  - As R increases the inner potential core decreases
  - At a short distance from jet exit each jet can be treated as separate jets
- Crow and Champagne, 1971
  - Single jet preferred mode "large-scale vortex puffs", $St_d=fd/U$~0.3
  - For Re:[10^2-10^3] instabilities go from sinusoid to helix to axisymmetric waves
  - Studied response to inline acoustics

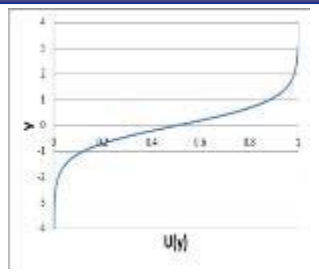

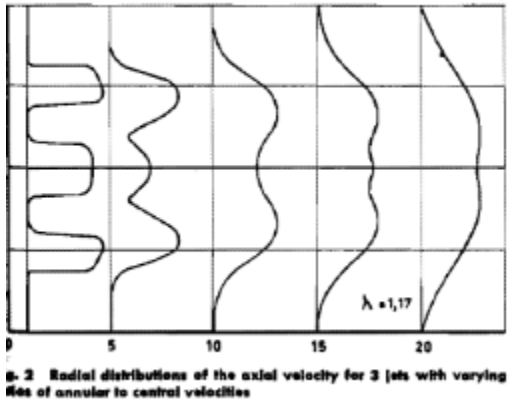

From Chigier NA. and Beer JM, The Flow Region Near the Nozzle in Double Concentric Jets, J of Basic Eng, 1964

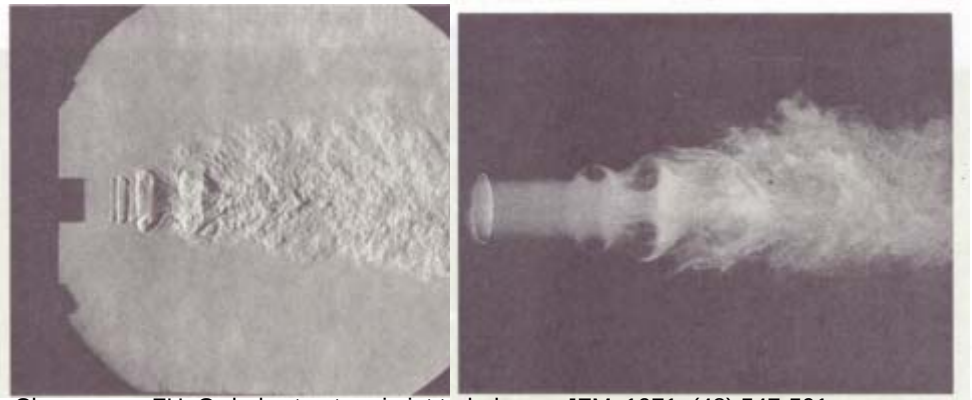

From Crow SC, Champagne FH, Orderly structure in jet turbulence, JFM, 1971, (48) 547-591

Earlier contributors to the field 2/2

- **Ko et al,1976-1989**
  - **Some of the most extensive earlier work by a single group on coaxial jet characterization**
  - **Very detailed description of near field mixing for coaxial jets. Many later authors cite his nomenclature**
  - **Similarity solutions, variation of St with axial distance**
  - **Development of vortex structures in the inner and outer shear layers**

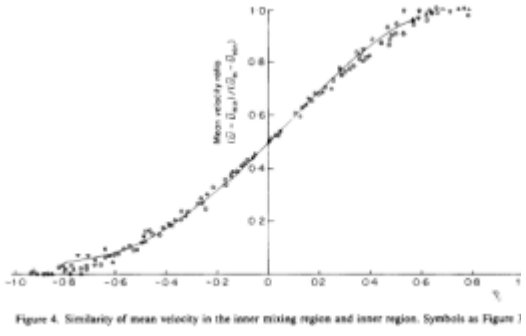

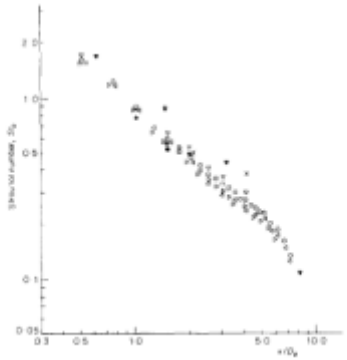

From [6]

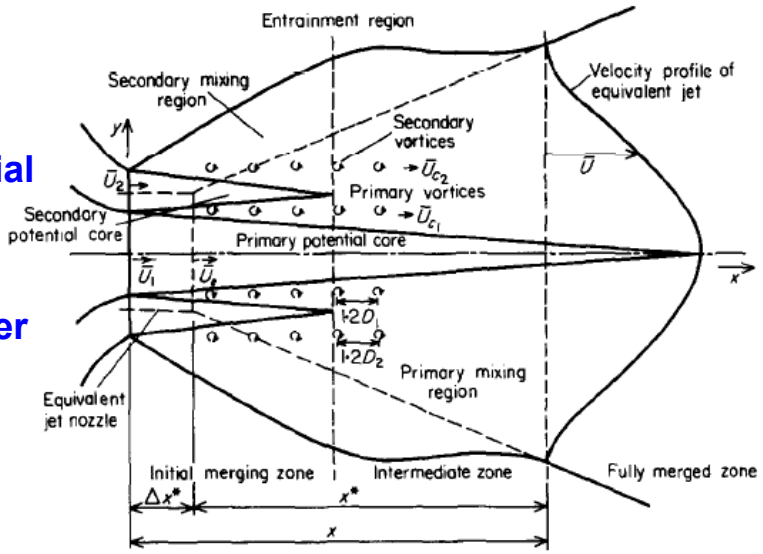

Kwan and Ko, J. Sound and Vibration, 48 (2), 1976

1. A. S. H. KWAN and N. W. M. Ko 1976 *Journal of Sound and Vibration 48, 203-219.* Coherent structures in subsonic coaxial jets.
2. Kwan ASH and Ko WM, J. Sound and Vibration, 48 (2), 1976, Coherent structures in subsonic coaxiial jets.
3. N. W. M. KO and A. S. H. KWAN 1976 *Journal of Fluid Mechanics 73,305332.* The initial region of subsonic coaxial jets.
4. Kwan, A. S. H. and Ko, N. W. M., "The Initial Region of Subsonic Coaxial Jets. Part II," *Journal of Fluid Mechanics,* Vol. 82, No. 2, 1977, pp, 273-287
5. Au, H. and Ko, N. W. M., "Coaxial Jets of Different Mean Velocity Ratios. Part 2," *Journal of Sound and Vibration,* Vol. 116, No. 3, 1987, pp. 427-443.
6. Ko NWM and H Au, "Coaxial Jets of Different Mean Velocity Ratios", *J of Sound and Vibration*, Vol 100 No. 2, 1985, 211-232

Highlights from previous work - 70s to early 80s

- **Boldman et al, 1975**
  - **Experimental and theoretical analysis for mixing of two air streams with different velocities – points out different vortex interactions, St_l~0.2 (U_{ave})**

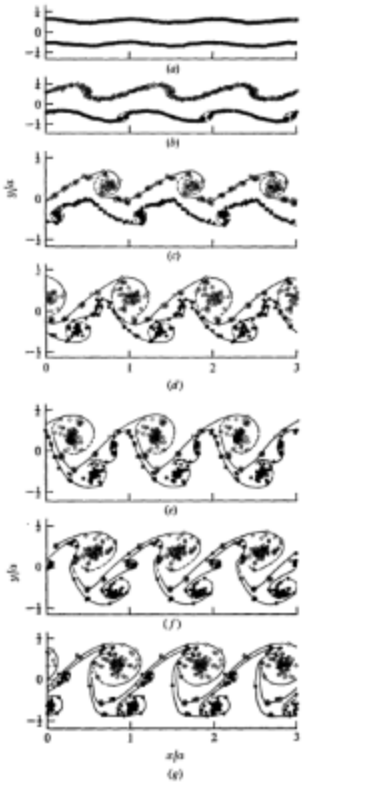

FIGURE 6. Point-vortex patterns at a velocity ratio $U_r = 0{\cdot}75$; $h/a = 0{\cdot}281$, $\bar{U} = 1{\cdot}0$, $A = -0{\cdot}0890$, $B = -0{\cdot}0749$, $N^+ = 84$, $N^- = 63$. (a)–(g) as in figure

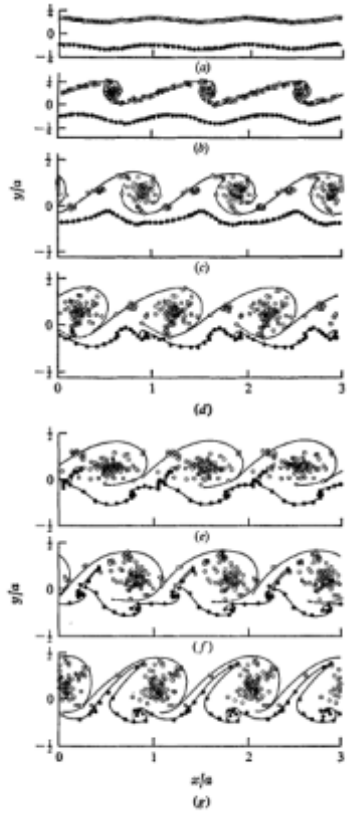

FIGURE 8. Point-vortex patterns at a velocity ratio $U_r = 0{\cdot}25$; $h/a = 0{\cdot}281$, $\bar{U} = 1{\cdot}0$, $A = -0{\cdot}0890$, $B = -0{\cdot}0749$, $N^+ = 84$, $N^- = 21$. (a)–(g) as in figure 5.

- Early analysis of what happens a recirculation zone when two streams separated by a blunt edge are of unequal velocities
- Even those the visualizations were not very clear the analysis captures the change in structures that later experiments will verify

From Boldman, D.R., Brinidh, P.F., and Goldstein, M.E., "Vortex Shedding from a Blunt Trailing Edge with Equal and Unequal External Mean Velocities," JFM, (75) 4, 1976, 721-735

- **Gutmark and Ho, 1983**
  - **Collects previous results on jet preferred mode, St_d has a range from ~0.24-0.64**

Highlights from previous work – early 90s

- Dahm et al, 1992
  - Studied different instabilities in the inner and outer shear layers plus effect of absolute velocity and R

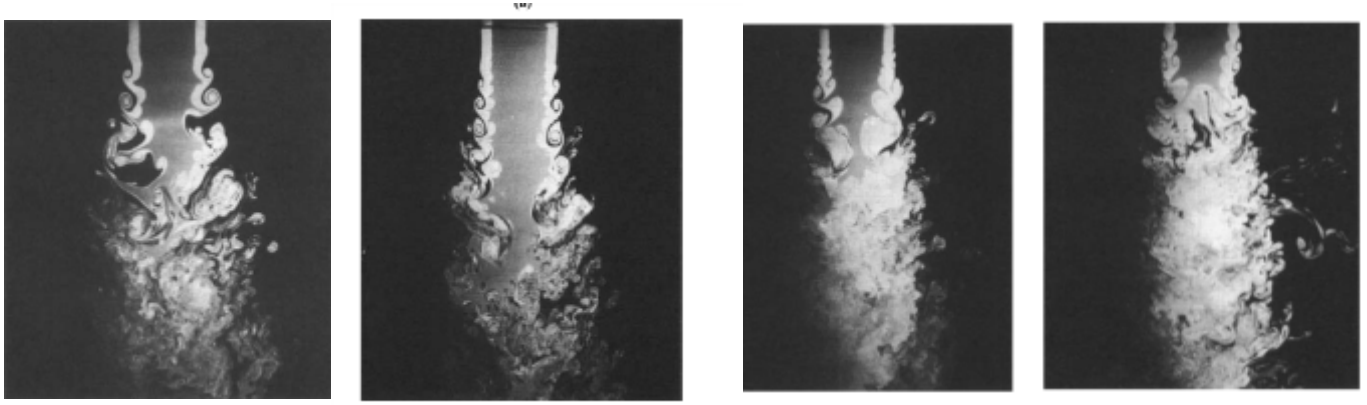

Dahm et al, JFM (241) 1992

R increases →

- Wicker and Eaton, 1994
  - Forces air inner and outer jets independently – observes vortex growth

Wicker and Eaton, AIAA J. (32) No.3.1994

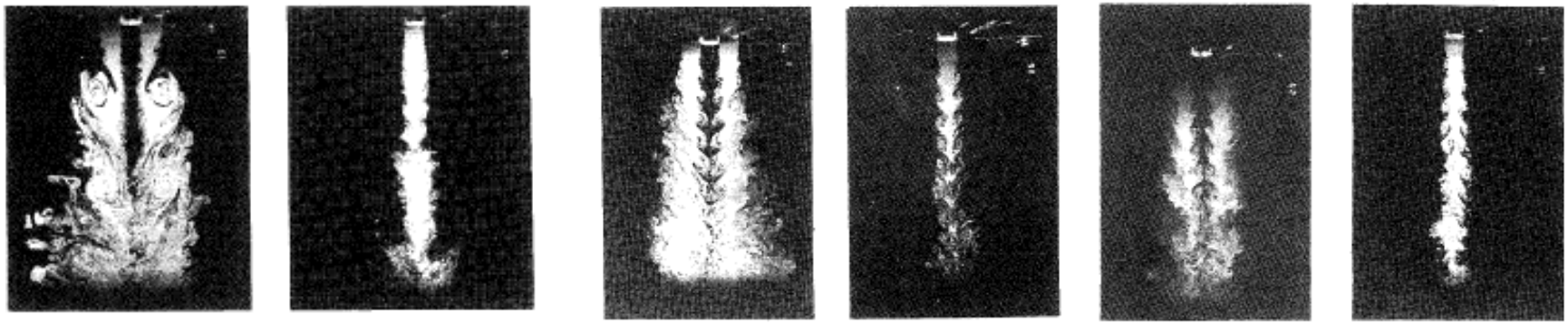

Fig. 7 $U_o/U_i = 0.55$, $U_i = 10$ m/s, $f_a = 48$ Hz, $St_{D_o} = 0.53$, $u_o'/U_o = 0.18$.

Fig. 11 $U_o/U_i = 0.55$, $U_i = 10$ m/s, $f_i = 375$ Hz, $St_{D_i} = 0.75$, u_i'/U_i Fig. 14 $U_o/U_i = 1.45$, $U_i = 10$ m/s, $f_i = 625$ Hz, $St_{D_i} = 1.18$, $u_i'/U_i = 0.022$. 0.052.

Highlights from previous work 90s –2000s

- **Buresti, Talamelli, Petagna (1994, 1998)**
  - **Air jets, same density, top-hat profile, $St_{do}=fd_o/U_{oj}$~0.3 to 1, function of x/D_i**

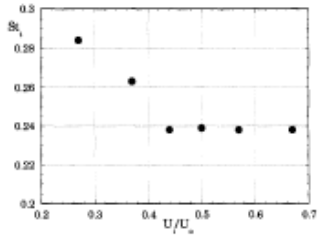

Figure 13. Variation of Strouhal number St_i with decreasing inner velocity.

Buresti et al, Exp Thermal and Fluid Science, 1994, 9:135-146

- **Balarac, da Silva, Metais et al (2003, 2007)**
  - **DNS analysis of coaxial jets - same density, top-hat profiles**
  - **Consider two shear layers, study effect of R**
  - **Consider axisymmetric and azimuthal excitation**

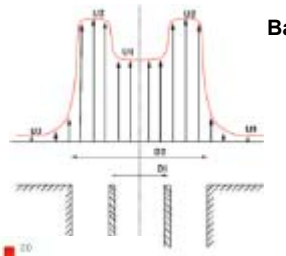

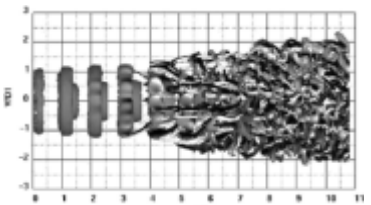

Balarac et al, Phys of Fluids (19), 2007

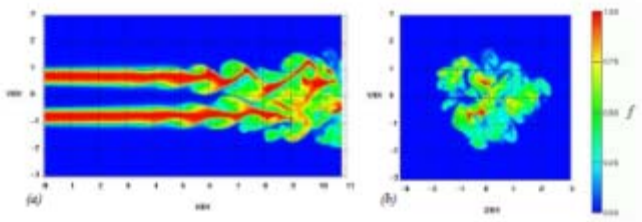

Figure 4. Instantaneous contours of mixture fraction for the DNS1O case: (a) in the central plane and (b) in the transverse section located at $x/D_1 = 10$. f varies from 0 (blue) to 1 (red) following the color scale shown in the figure.

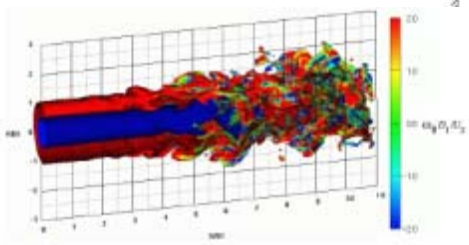

Figure 28. Cut view of $f = 0.5$ mixture-fraction isosurface colored by the tangential vorticity ω_θ following the color scale shown on the figure, for DNS10.

Balarac et al, J of Turbulence, 2007

- **Segalini, Talamelli, et al (2006, 2011)**
  - **Air jets, same density, top-hat profile, $St_{b(lip)}=fb(lip)/U_{average}$**

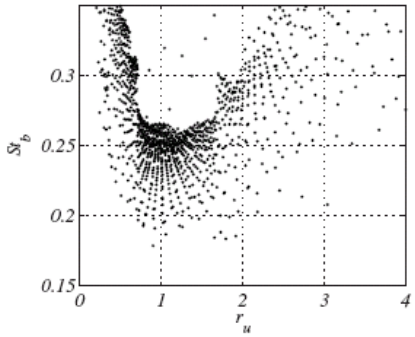

Segalini et al, Phys of Fluids (23), 2011

Highlights from previous work, late 2000s

- **Birbaud, Ducruix, Durox, Candel (2006-2007)**
  - **Single air jets, low Re, laminar, top-hat profile, subjected to acoustic modulation**
  - **Systematic study of effect of modulation in terms of St_d, St_θ**
  - **Need similar study for shear coaxial jets**

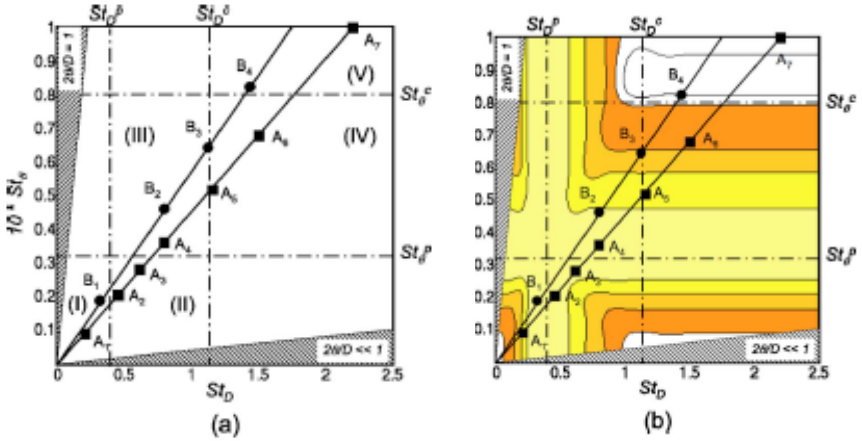

Birbaud et al, Phys of Fluids (19), 2007

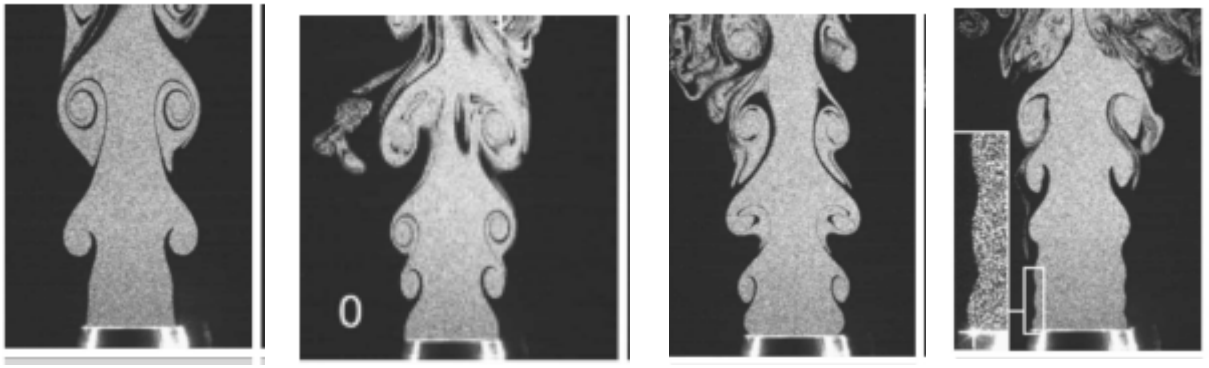

Highlights from previous work late 2000s to today

- **Richecoeur, Scouflaire, Ducruix, Candel (2006)**
  - **Forced transverse acoustic excitation of flames**

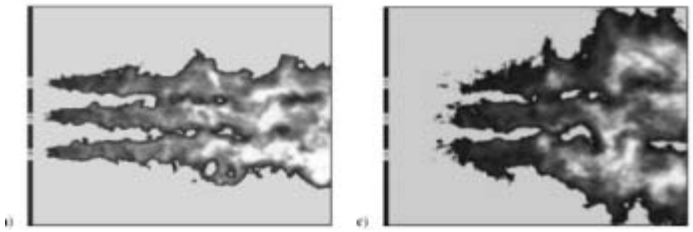

Richecoeur et al, JPP (22) No 4, 2006

- **Kastengren et al 2013**
  - **X-ray radiography used to quantitatively examine shear coaxial jet injectors First quantitative measurement of the mass density in the near injector region of this injector type. Centerline EPL profiles showed same general trend with J reported in studies of the dark core length. Shortening of the core region with increasing J.**

AFRL's previously published research on shear coaxial jets: non-reacting studies

- **Study the mixing process and response to external acoustic perturbations for shear-coaxial injectors typically used in cryogenic engines**
  - Investigate influence of injector geometry
  - Vary the outer-to-inner jet momentum flux ratio, J for P_r<1 and P_r>1

$$P_r = \frac{P_{chamber}}{P_{critical,\mathrm{N}_2}} \quad P_{critical,\mathrm{N}_2} = 3.4MPa\ (493\ psi)$$

  - Characterize mixing using dark-core length measurements
  - Apply proper orthogonal decomposition of high-speed image pixel intensity fluctuations to extract spatial and temporal characteristics of flow structures

Image of experimental facility

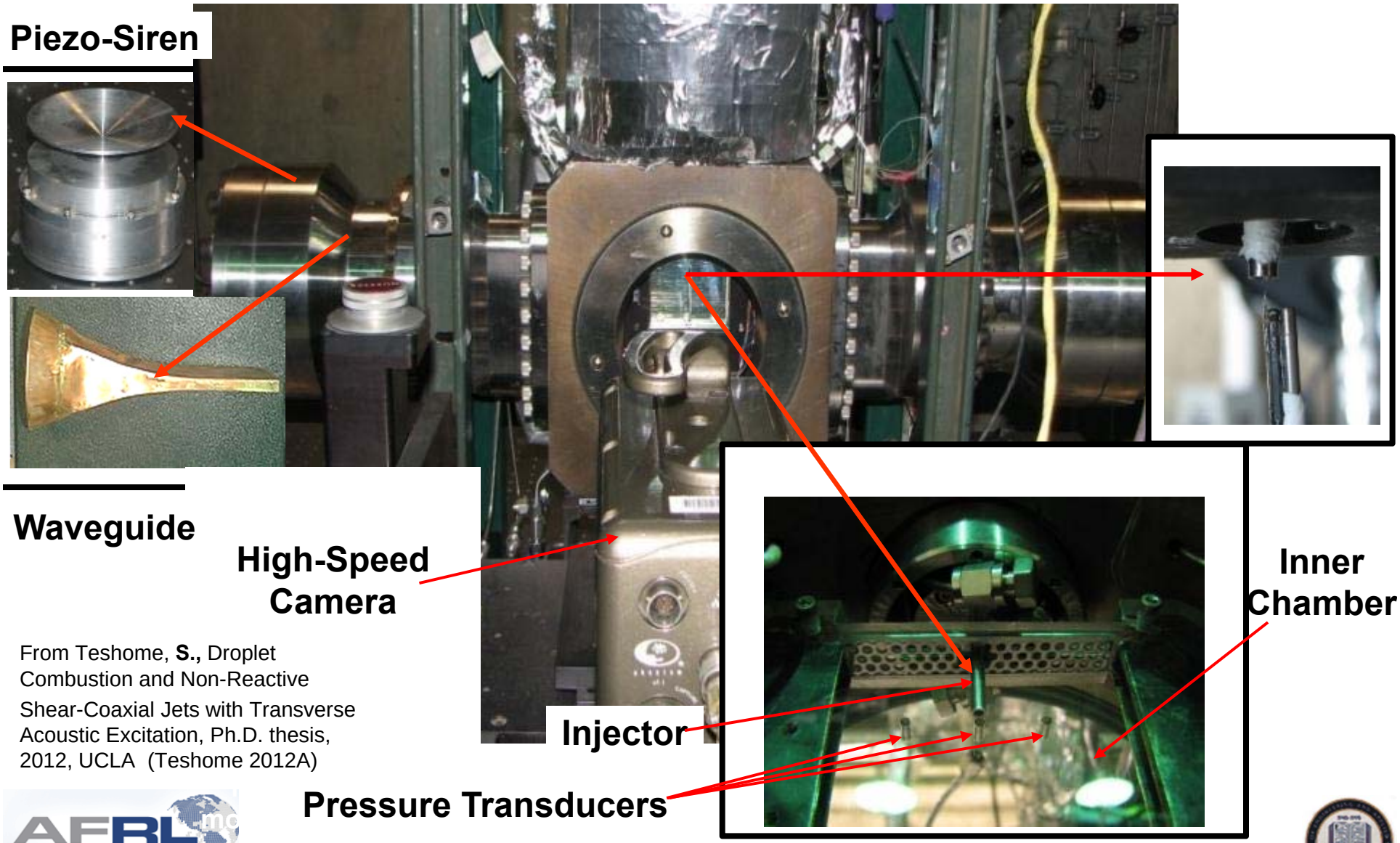

From Teshome, **S.,** Droplet Combustion and Non-Reactive Shear-Coaxial Jets with Transverse Acoustic Excitation, Ph.D. thesis, 2012, UCLA (Teshome 2012A)

Schematic of experimental facility

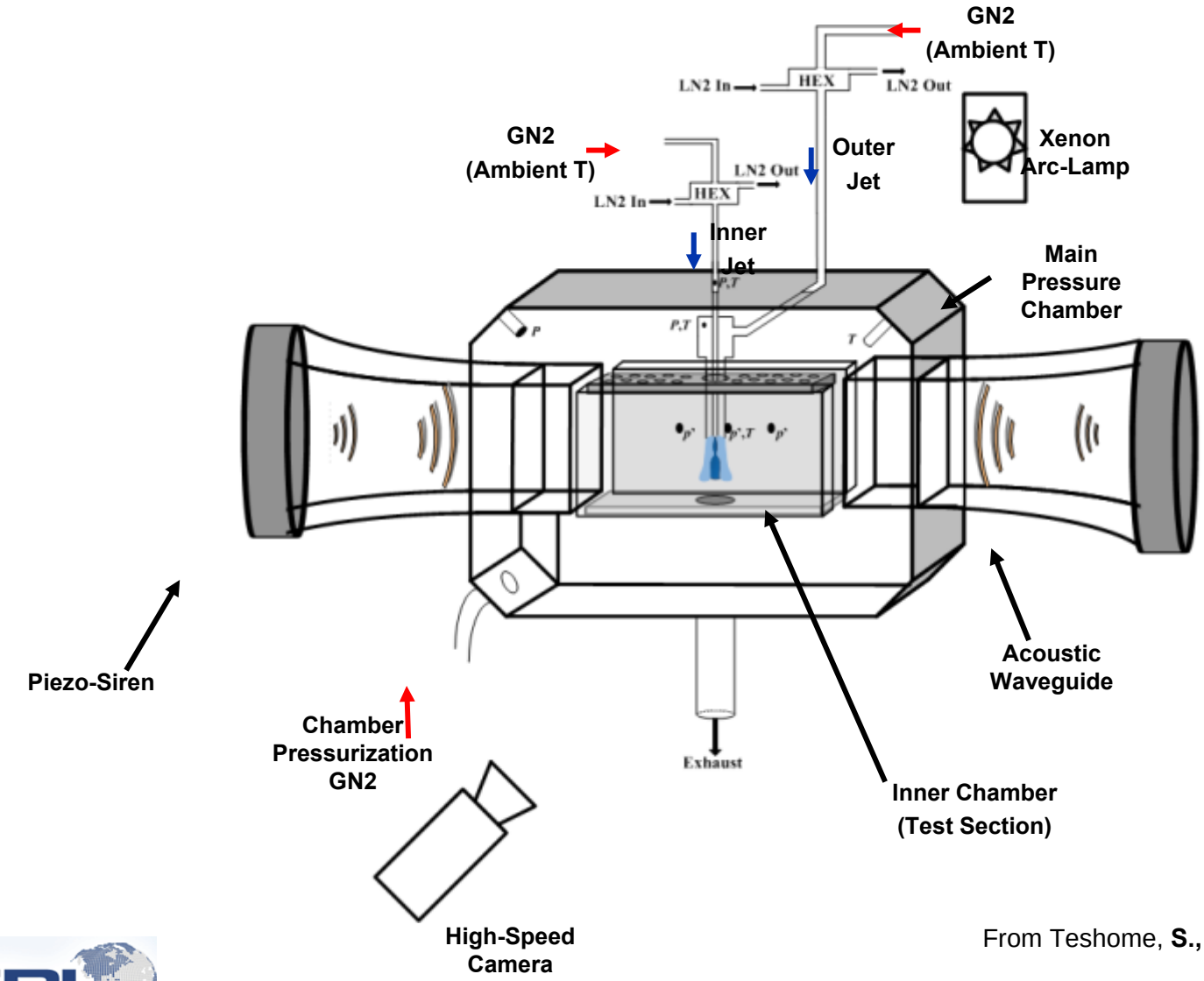

From Teshome, **S.**, 2012A

Density gradients around critical point of nitrogen

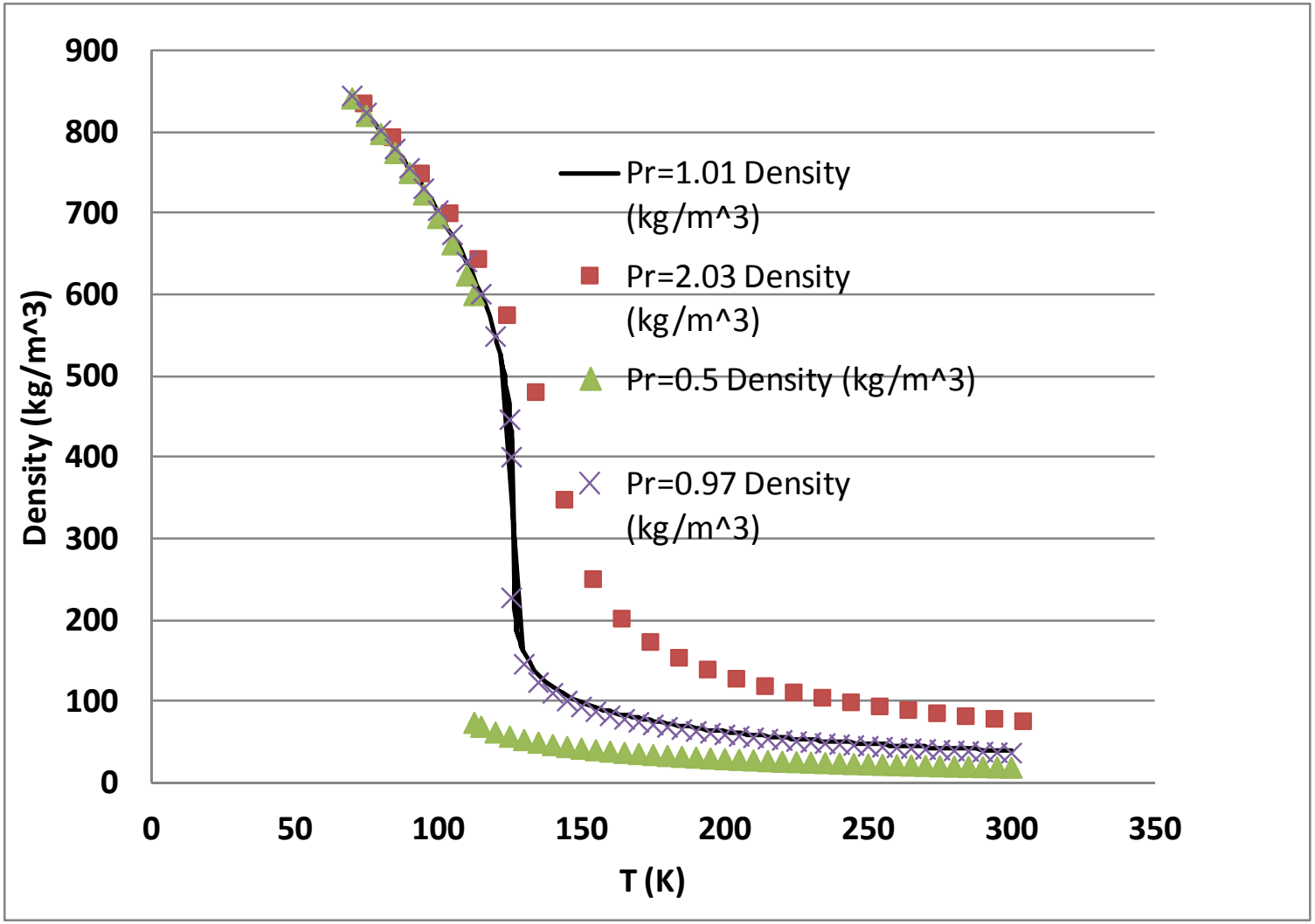

From http://webbook.nist.gov/chemistry/

Four geometric configurations studied

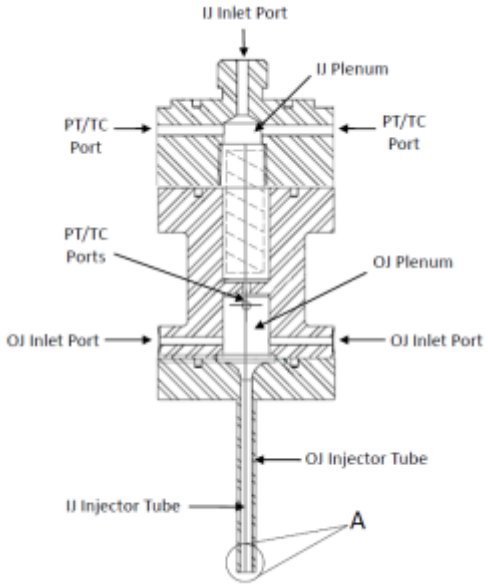

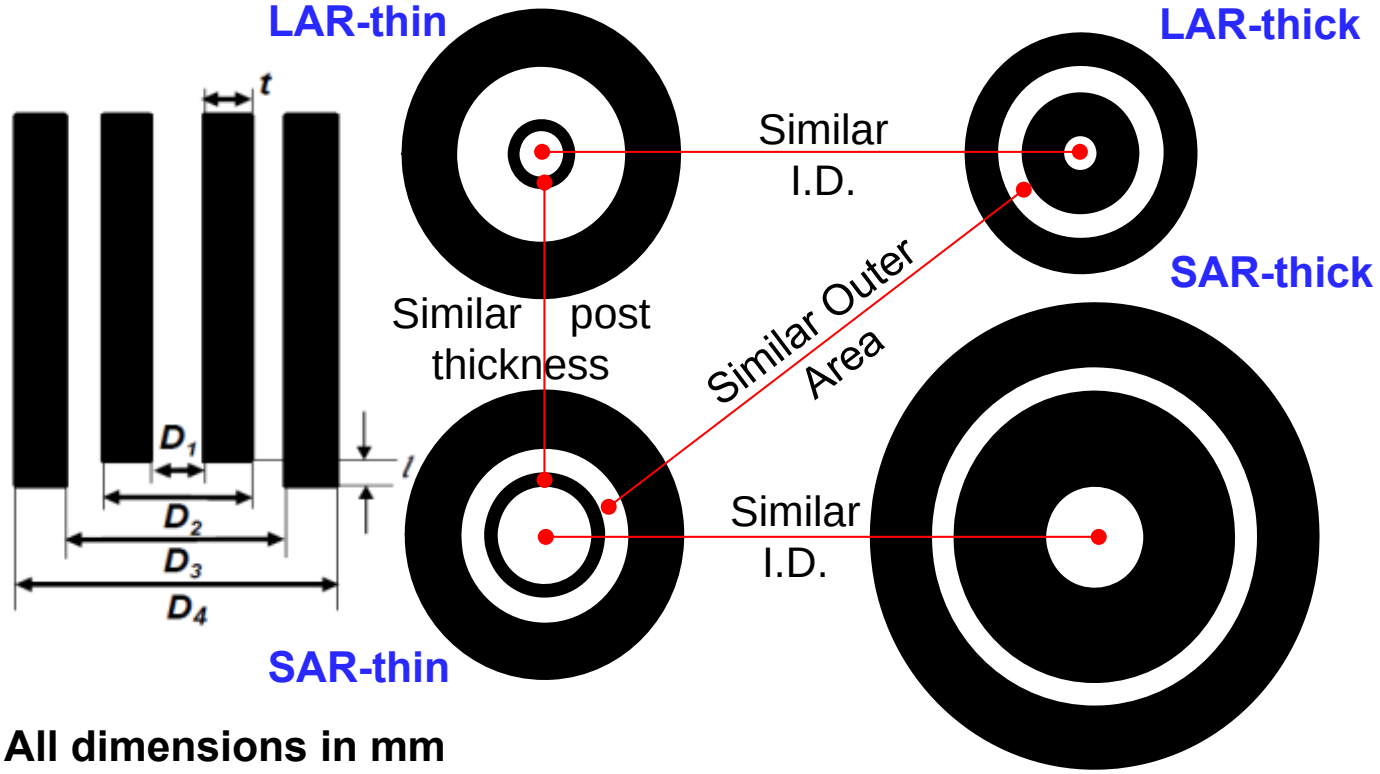

All dimensions in mm

Injector	D_1	D_2	D_3	D_4	t/D_1	A_o/A_i	l/D_1
LAR-thick	0.51	1.59	2.42	3.18	1.05	12.9	0.5
SAR-thin	1.40	1.65	2.44	3.94	0.09	1.6	0,0.5
SAR-thick	1.47	3.96	4.70	6.35	0.84	2.9	0.5
LAR-thin	0.70	0.89	2.44	3.94	0.13	10.6	-0.2

SAR, LAR → Small, Large Area Ratio

Thick, Thin → Post thickness

From S. Teshome, I.A. Leyva, J. Rodriguez, D. Talley, Geometry Effects on Steady and Acoustically Forced Shear-Coaxial Jet Sprays, ICLASS, 2012

Dark-core length measurement

- First raw grayscale images were converted to binary images
- A contour was drawn around the “dark-column” in the binary image
- Axial length of the dark-column measured and defined as the Dark-Core Length, *L*

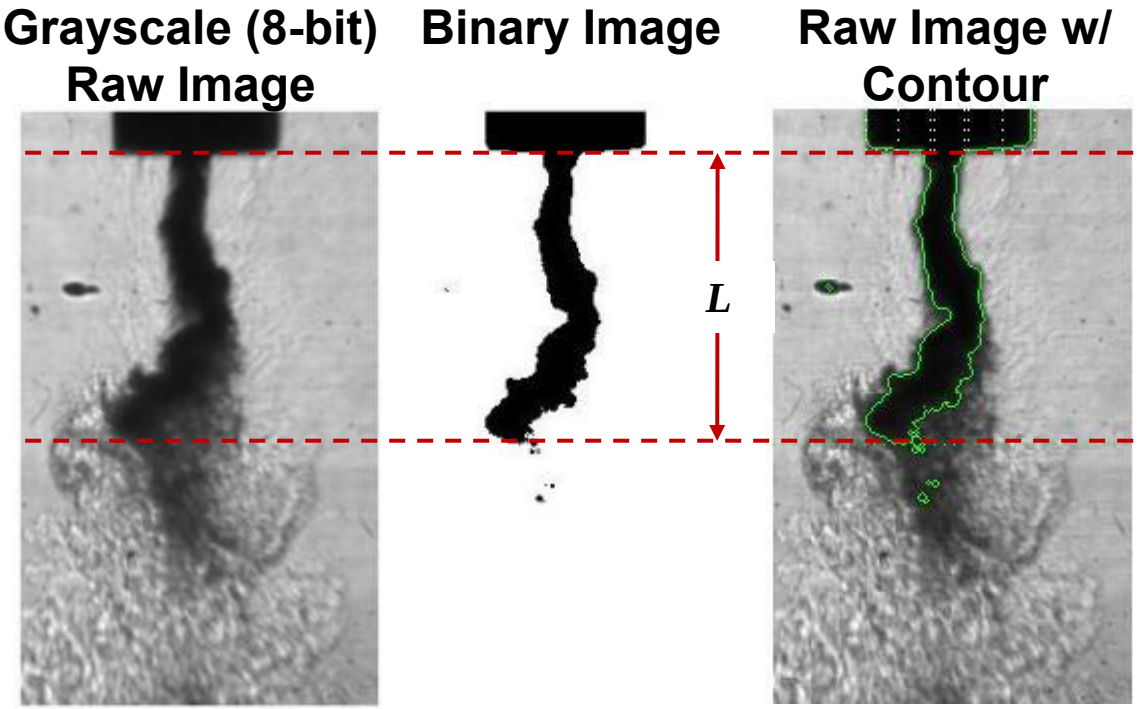

From Teshome 2012A

Break-up regimes for shear coaxial jets

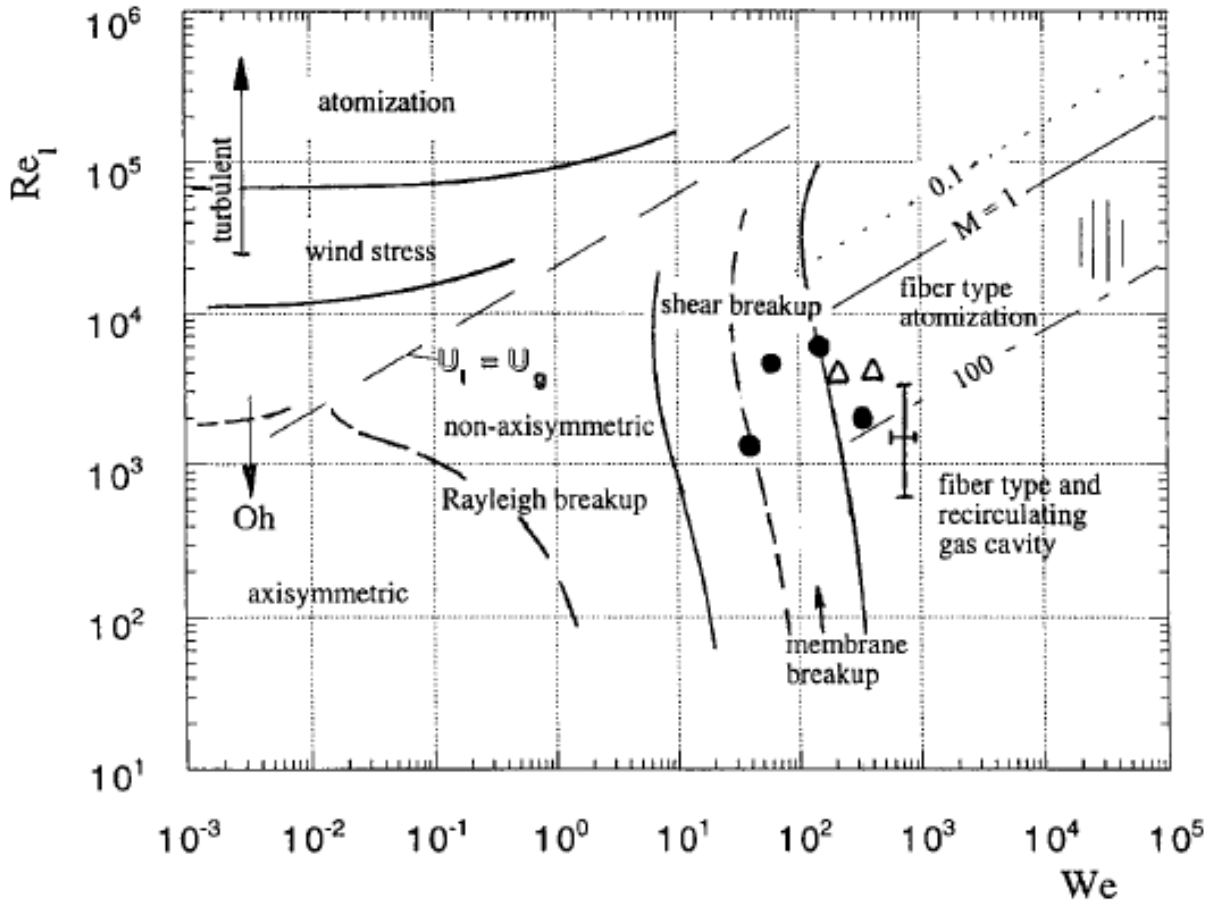

From Lasheras, J. C., and Hopfinger, E. J., "Liquid Jet Instability and Atomization in a Coaxial Gas Stream," Annual Rev. Fluid Mech., Vol. 32, 2000, pp. 275-308.

Different correlations for inner jet break-up length

REF	Author	Diagnostic	Quantity Measured	Equation
[58]	Lasheras et al.[g]	Photo-graph	Liquid intact length	$L/D_1 = \left(\frac{1}{4(C\alpha)^2 M} - \frac{1}{4}\right)^{1/2} \approx \frac{6}{M^{1/2}}$
[54]	Lasheras & Hopfinger [g,i]	i	i	$L/D_1 = \frac{1}{2cM^{2/3}}\left(\frac{\sigma}{\mu_i U_i}\right)^{1/3}$ $L/D_1 \approx \frac{6}{M^{1/2}}\left(\left\|1-\frac{U_i}{U_o}\right\|\right)^{-1}$ $L/D_1 \approx \frac{6}{M^{1/2}}\frac{1}{\left(1-\frac{B\sigma}{\mu_o U_o}\right)^{0.5}}$
[60]	Favre-Marinet & Schettini	Aspirating Probe w/ hot-wire	Potential Core	$L/D_1 \propto M^{-0.5}$
[65]	Porcheron et al.	Fiber optic Probe	Liquid Core	$L/D_1 = 2.85\left(\frac{\rho_o}{\rho_i}\right)^{-0.38} Z^{0.34} M^{-0.13}$
This work	Davis	Shadow-graph	Dark Core	$L/D_1 \approx \frac{12}{M^{1/2}}$ $L/D_1 \approx \frac{25}{M^{0.2}}$

From D.W. Davis. On the Behavior of a Shear-Coaxial Jet, Spanning Sub- to Supercritical Pressures, with and without an Externally Imposed Transverse Acoustic Field. Ph.d. dissertation, Pennsylvania State University, 2006.

[58] Lasheras, J. C, Villermaux, E., and Hopfinger, E. J., "Breakup and Atomization of a Round Water Jet by a High Speed annular Air Jet," JFM. (357) 1998, pp. 351-379.

[54] Lasheras, J. C., and Hopfinger, E. J., "Liquid Jet Instability and Atomization in a Coaxial Gas Stream," Annual Rev. Fluid Mech., Vol. 32, 2000, pp. 275-308.

[60] Favre-Marinet, M., and Camano Schettini, E. B., "The Density Field of Coaxial Jets with Large Velocity Ratio and Large Density Differences," International Journal of Heat and Mass Transfer, Vol. 44, 2001, pp. 1913-1924.

[65] Porcheron, E.., Carreau, J. L., Prevost, L., LeVisage, D., and Roger, F., "Effect of Density on Coaxial Liquid Jet Atomization," Atomization and Sprays, Vol. 12, 2002, pp. 209-227.

State of the art for mixing in shear coaxial jets - 2007

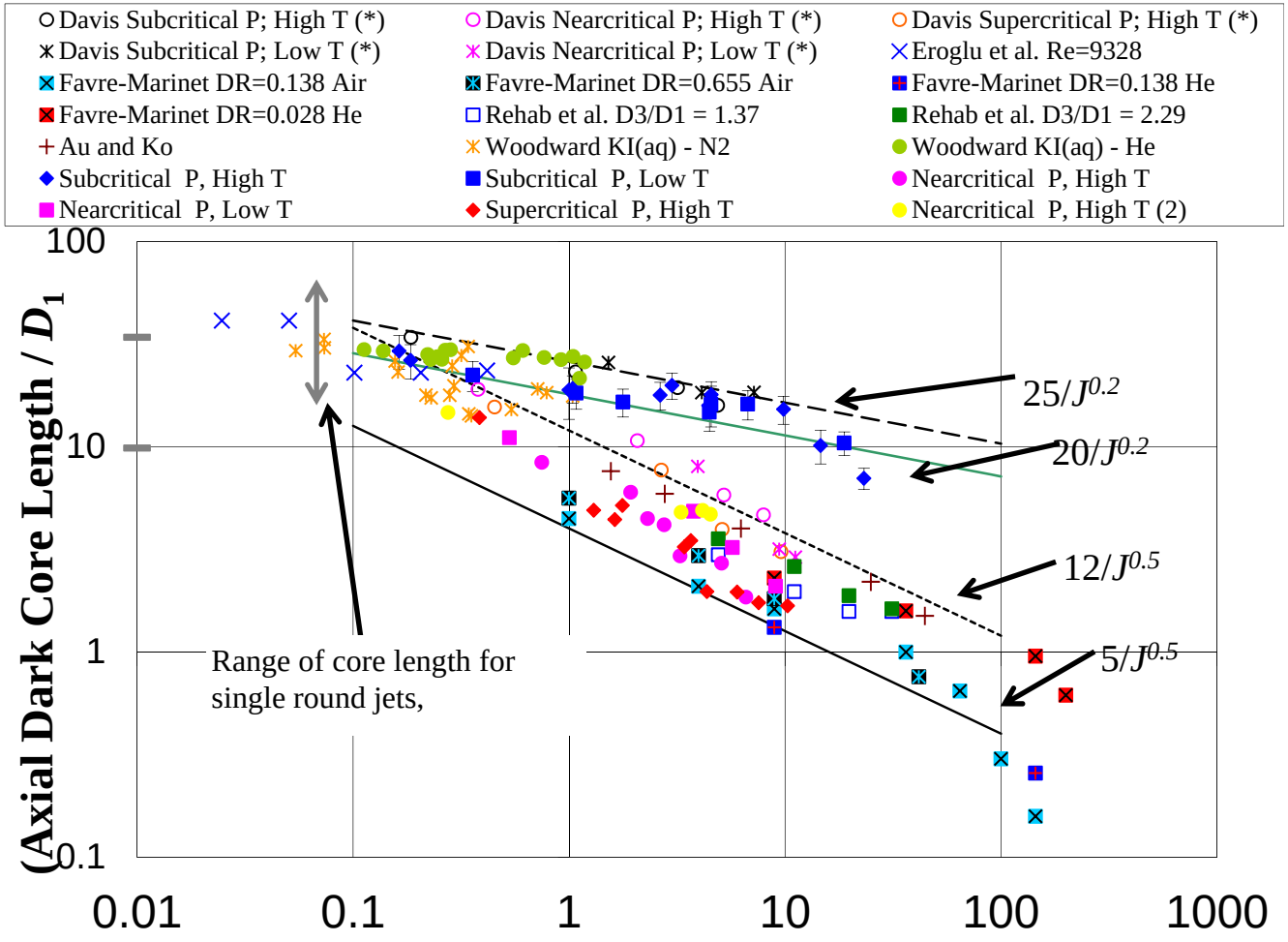

From: I. Leyva, B. Chehroudi, D. Talley, Dark Core Analysis of Coaxial Injectors at Sub-, Near-, and Supercritical Conditions in a Transverse Acoustic Field, AIAA 2007-5456

Differences between 2-phase and 1-phase coaxial jets

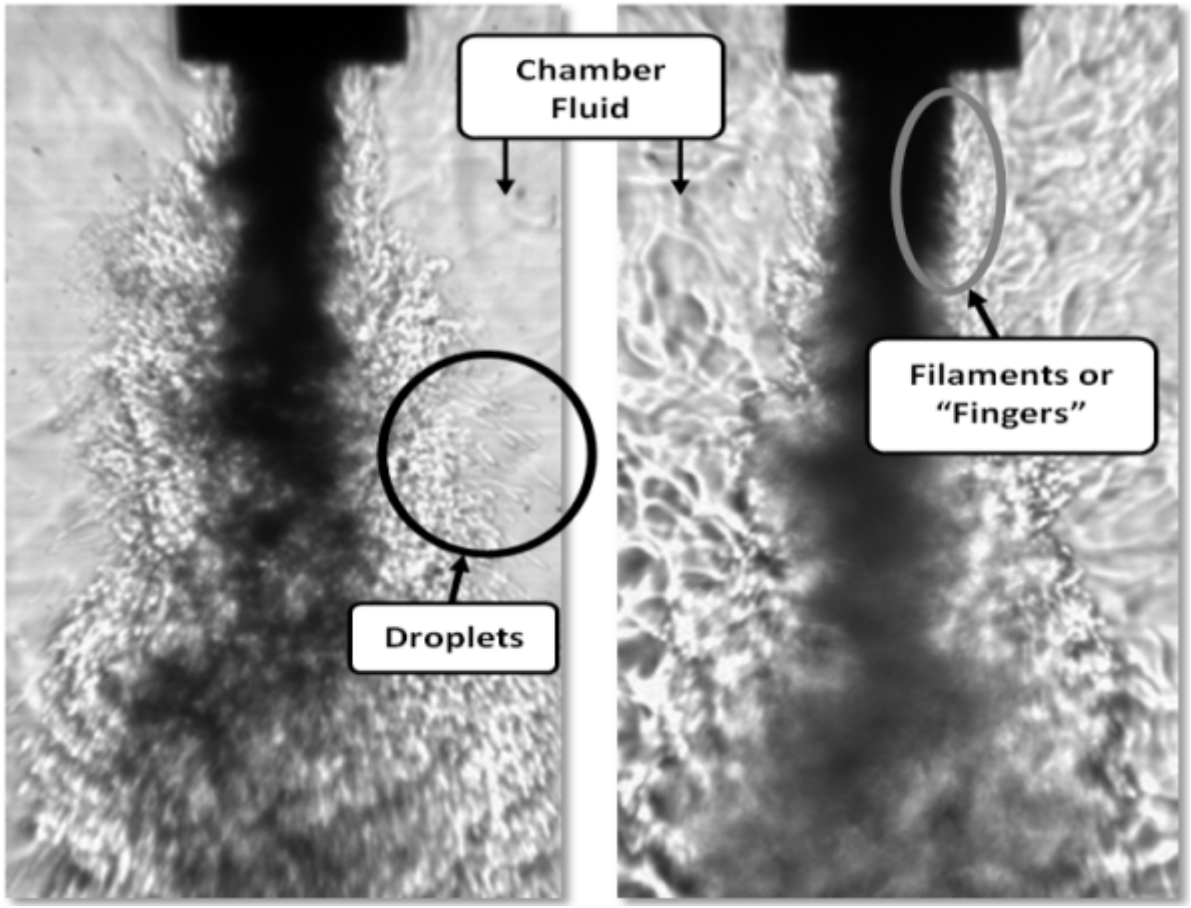

Pr=0.44 J~10 **Pr=1.05 J~10**

From J. I. Rodriguez. Acoustic Excitation of Liquid Fuel Droplets and Coaxial Jets. Ph.D. dissertation, UCLA, 2009.

Effect of acoustics on a single injector geometry

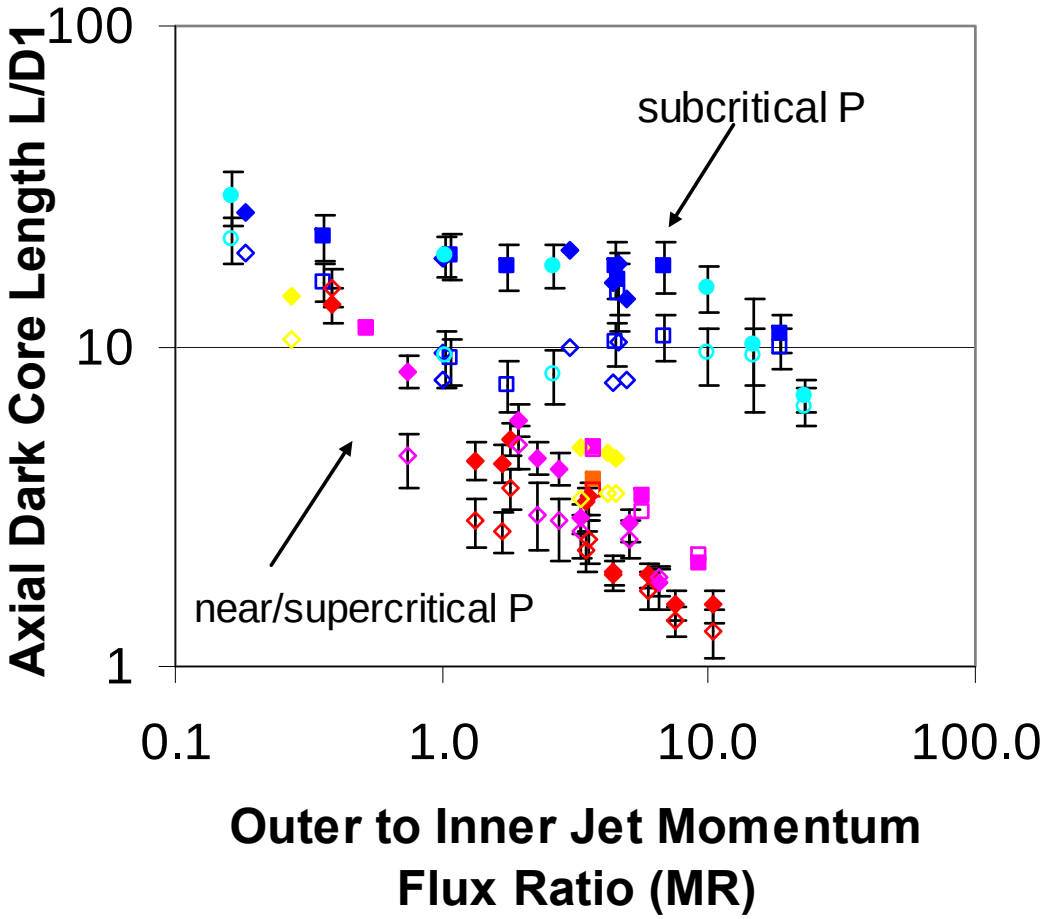

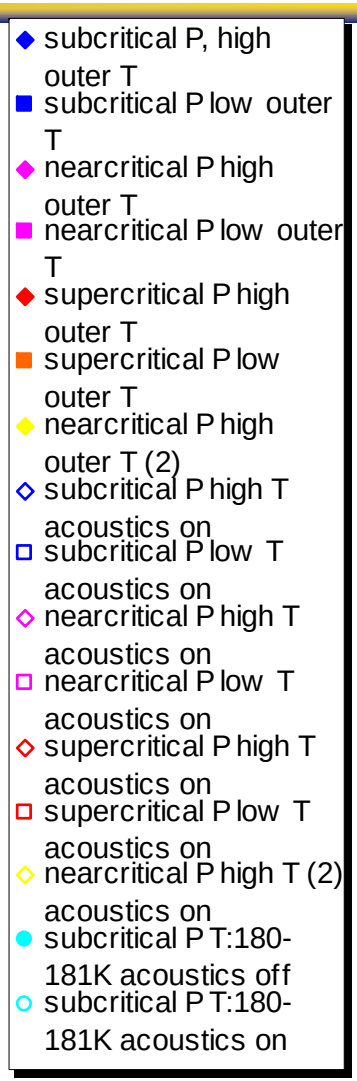

From: I. Leyva, B. Chehroudi, D. Talley, Dark Core Analysis of Coaxial Injectors at Sub-, Near-, and Supercritical Conditions in a Transverse Acoustic Field, AIAA 2007-5456

Baseline dark-core lengths for 4 geometries for $P_r = 0.44$

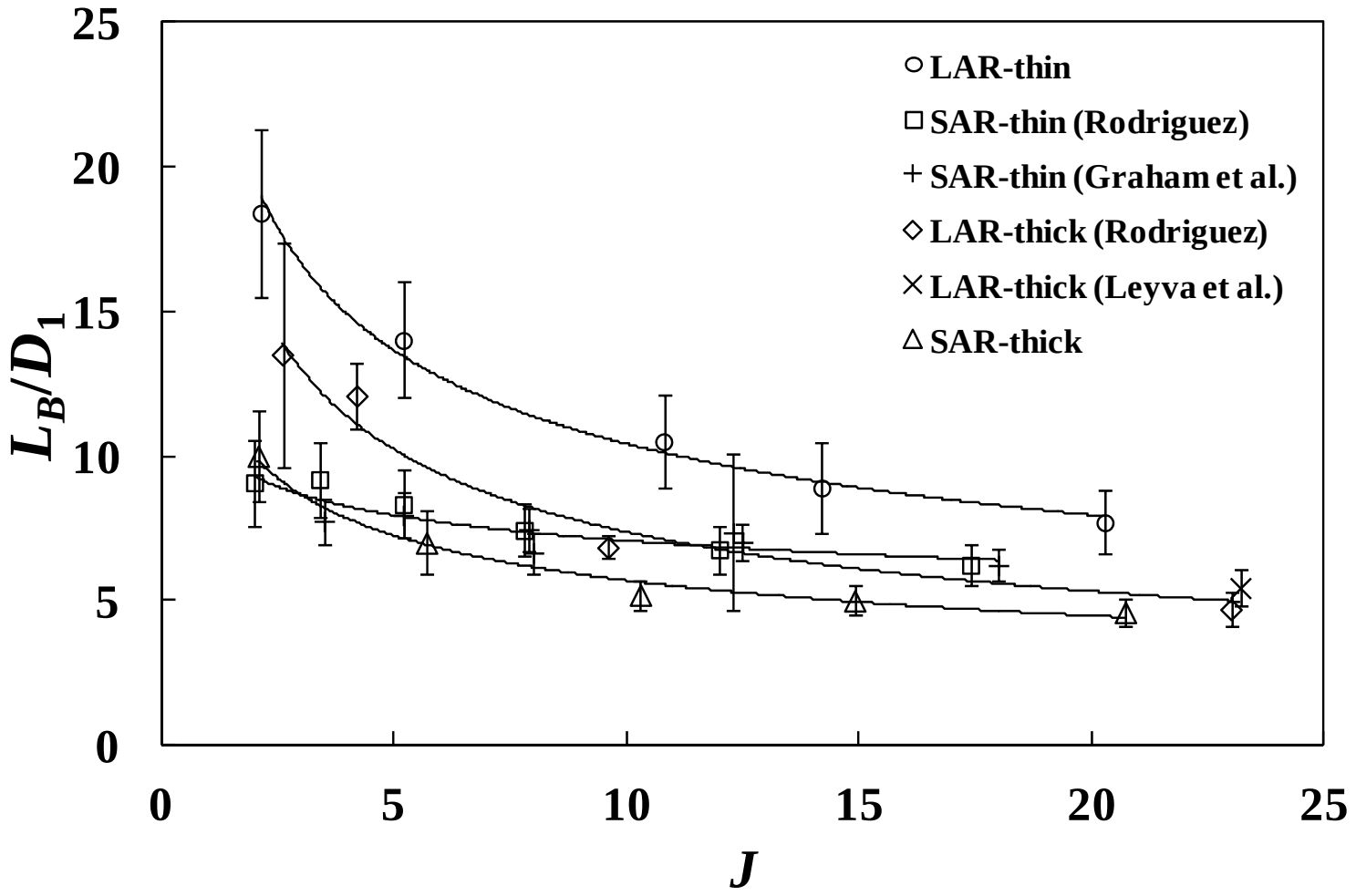

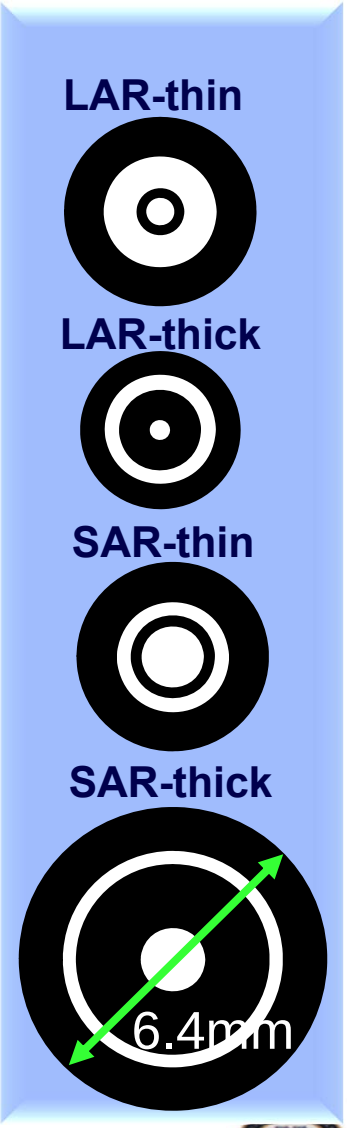

Fastest Mixing for SAR-thick – Slowest Mixing for LAR-thin

From Teshome 2012A

Baseline normalized DCL, L_B/D_1 – $P_r = 0.44$

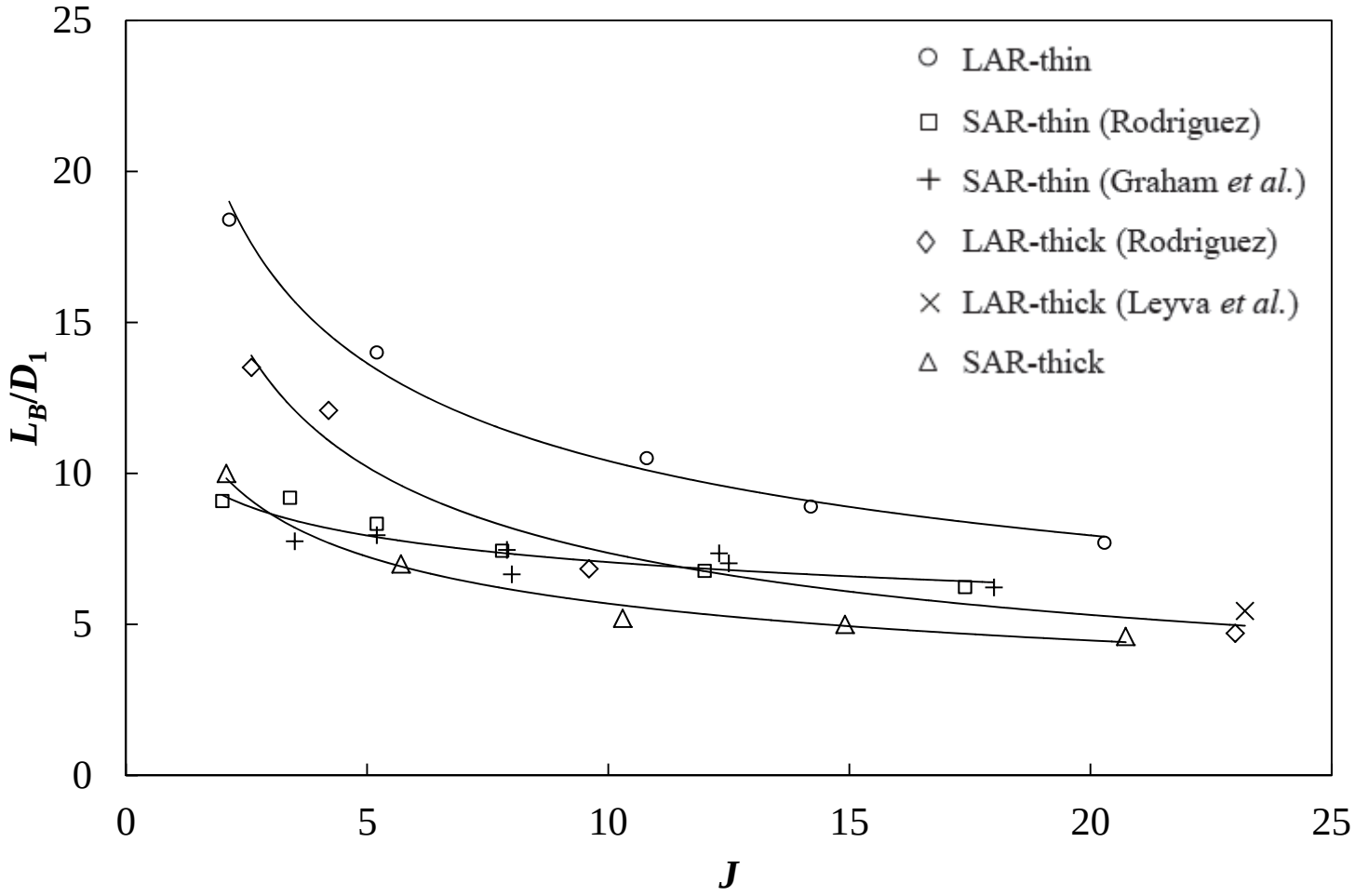

From Teshome 2012A

Baseline flows at $P_r = 0.44$

LAR-thin Injector

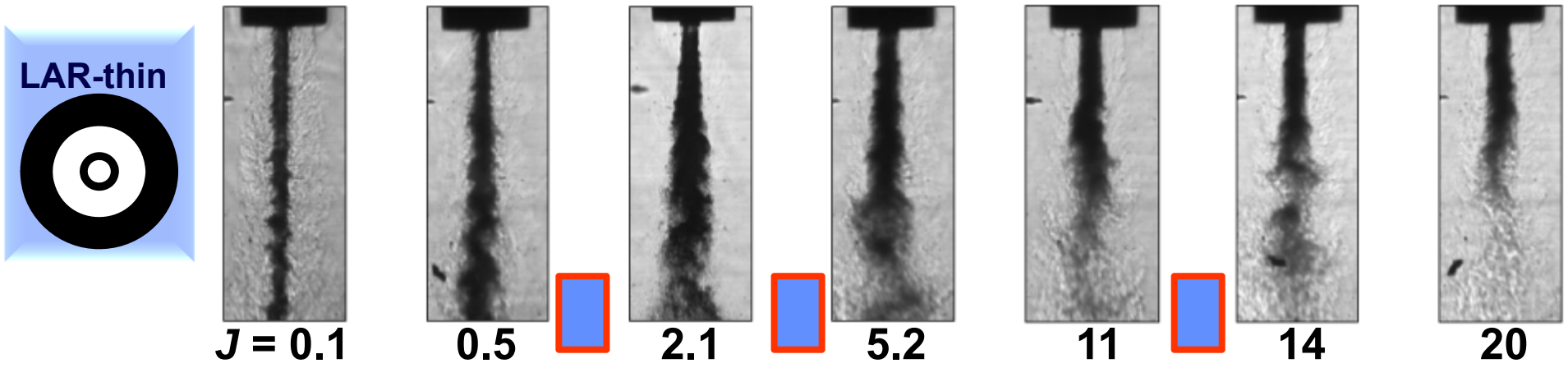

SAR-thick Injector

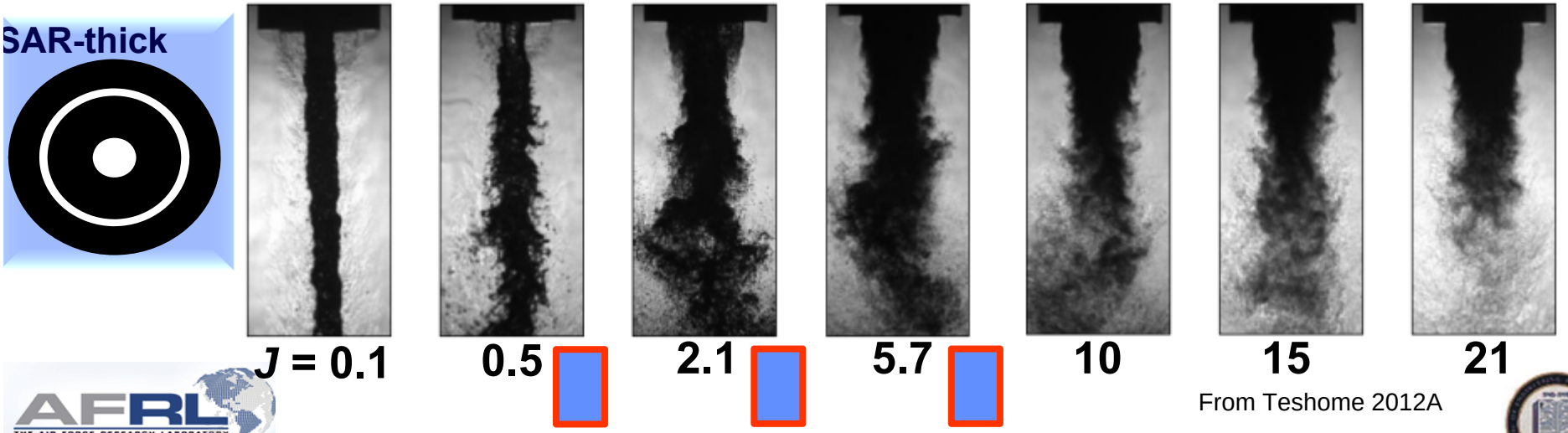

From Teshome 2012A

Baseline normalized DCL, L_B/D_1 – $P_r = 1.05$

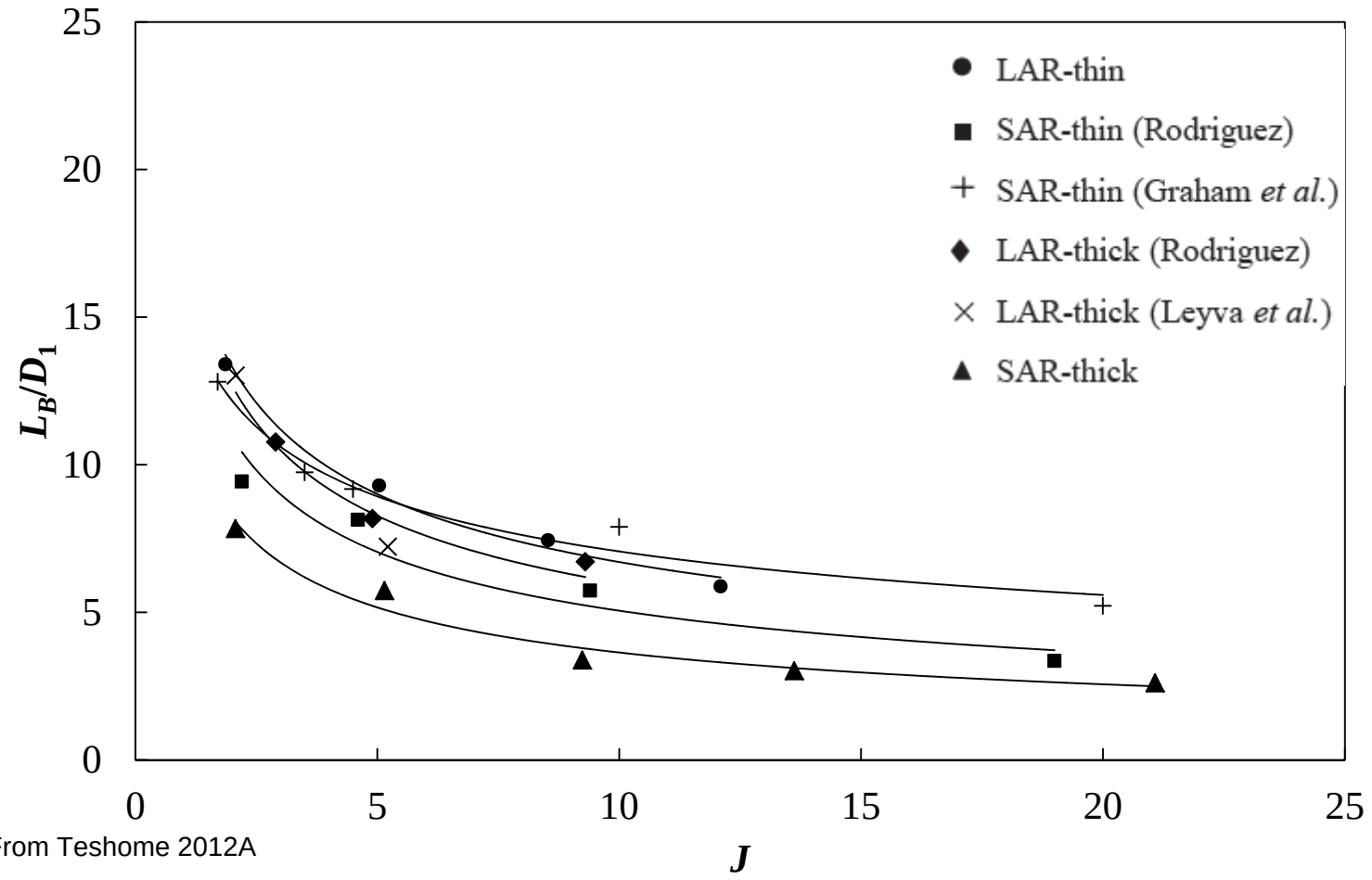

From Teshome 2012A

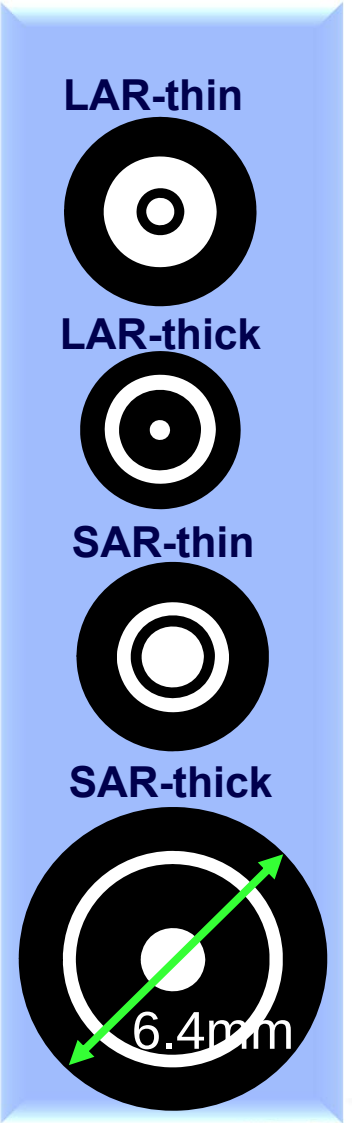

Baseline flows at $P_r = 1.05$

LAR-thin Injector

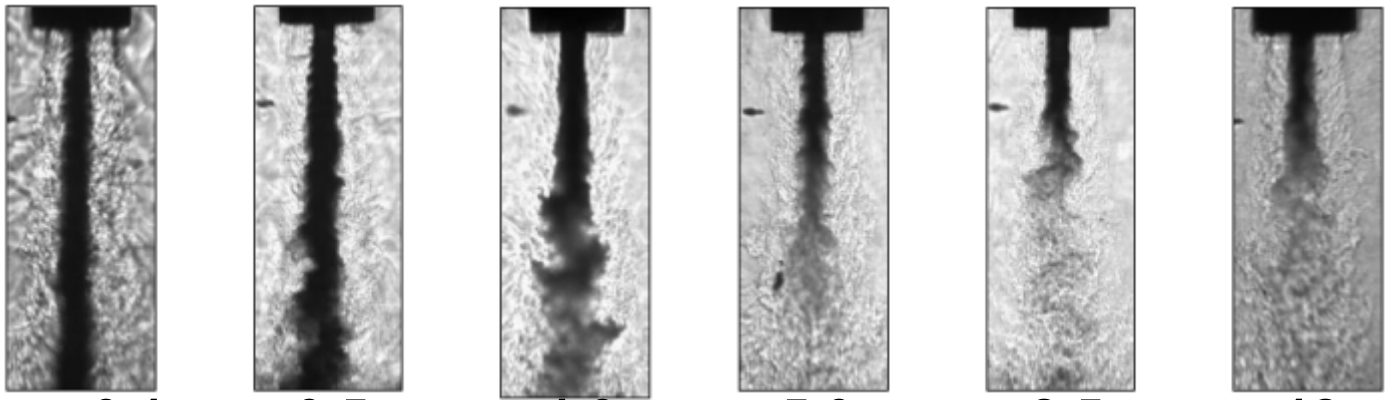

SAR-thick Injector

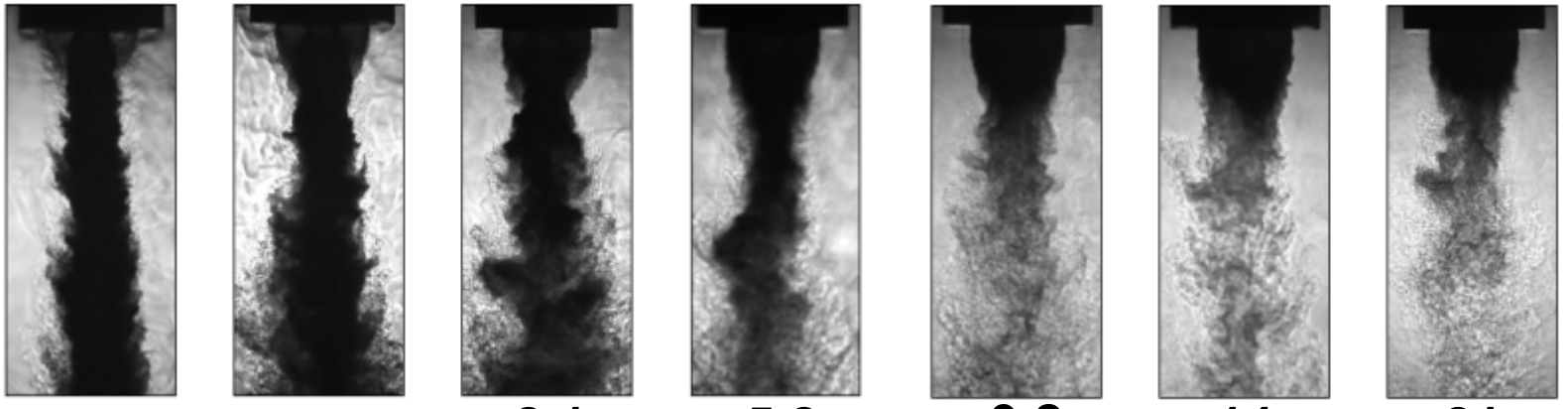

From Teshome 2012A

Baseline normalized DCL, L_B/D_1 collapse

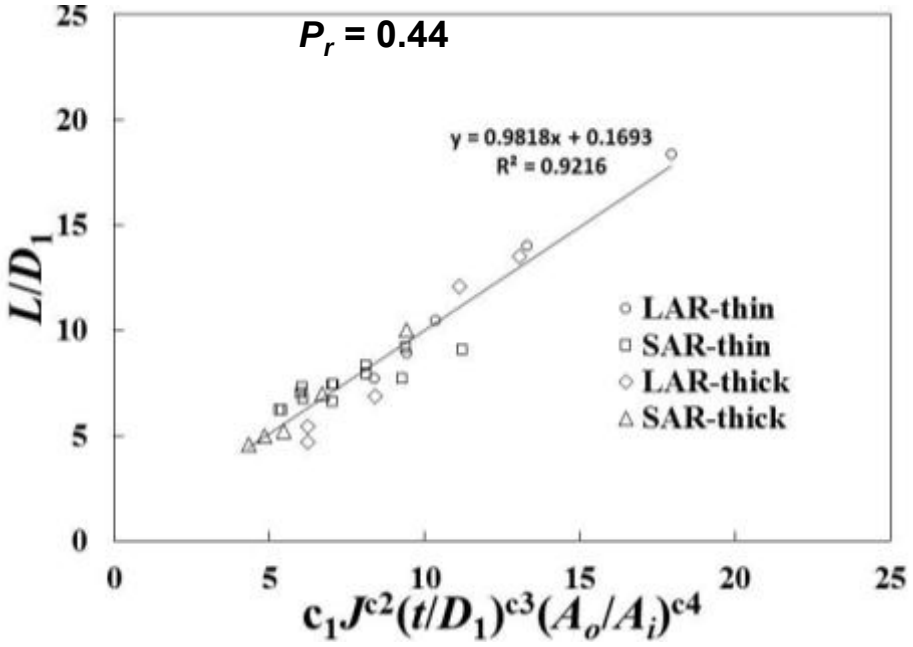

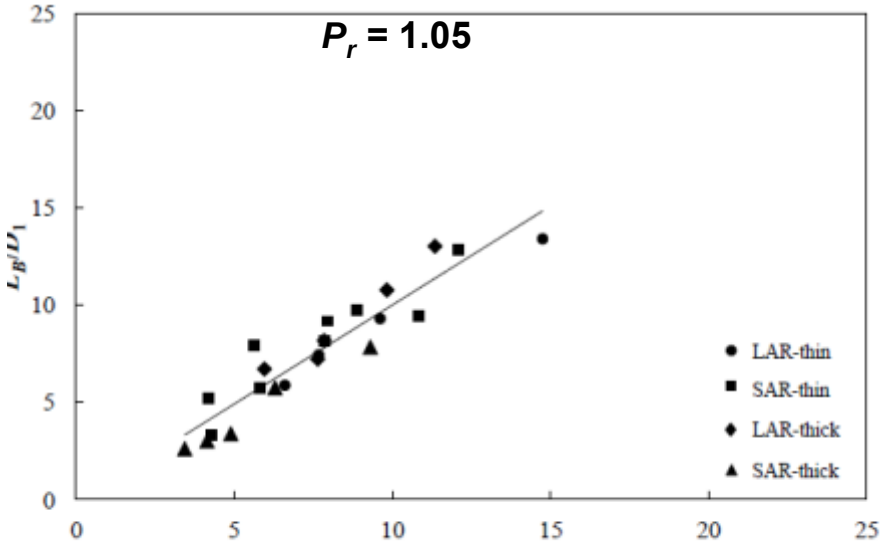

$$c_1 J^{c2} \left({}^{t}/_{D_1}\right)^{c3} \left({}^{A_o}/_{A_i}\right)^{c4}$$

P_r	c_1	c_2	c_3	c_4
0.44	9	-0.34	-0.15	0.30
1.05	11	-0.43	-0.12	0.15

$$\left(\frac{L}{D_1}\right) = c_1 J^{c2} \left(\frac{t}{D_1}\right)^{c3} \left(\frac{A_o}{A_i}\right)^{c4}$$

Has characterized mixing for shear coaxial injectors taking into account geometry and flow conditions!

From Teshome 2012A

ACOUSTIC EXCITATION ANALYSIS

Acoustic field set-up: pressure antinode

- Pressure antinode (PAN) – condition of maximum pressure perturbation in the acoustic field
- Piezo-sirens forced in-phase
- Superposition of quasi-1D acoustic waves traveling in opposite directions ⇒ PAN at the jet location (geometric center of test section)

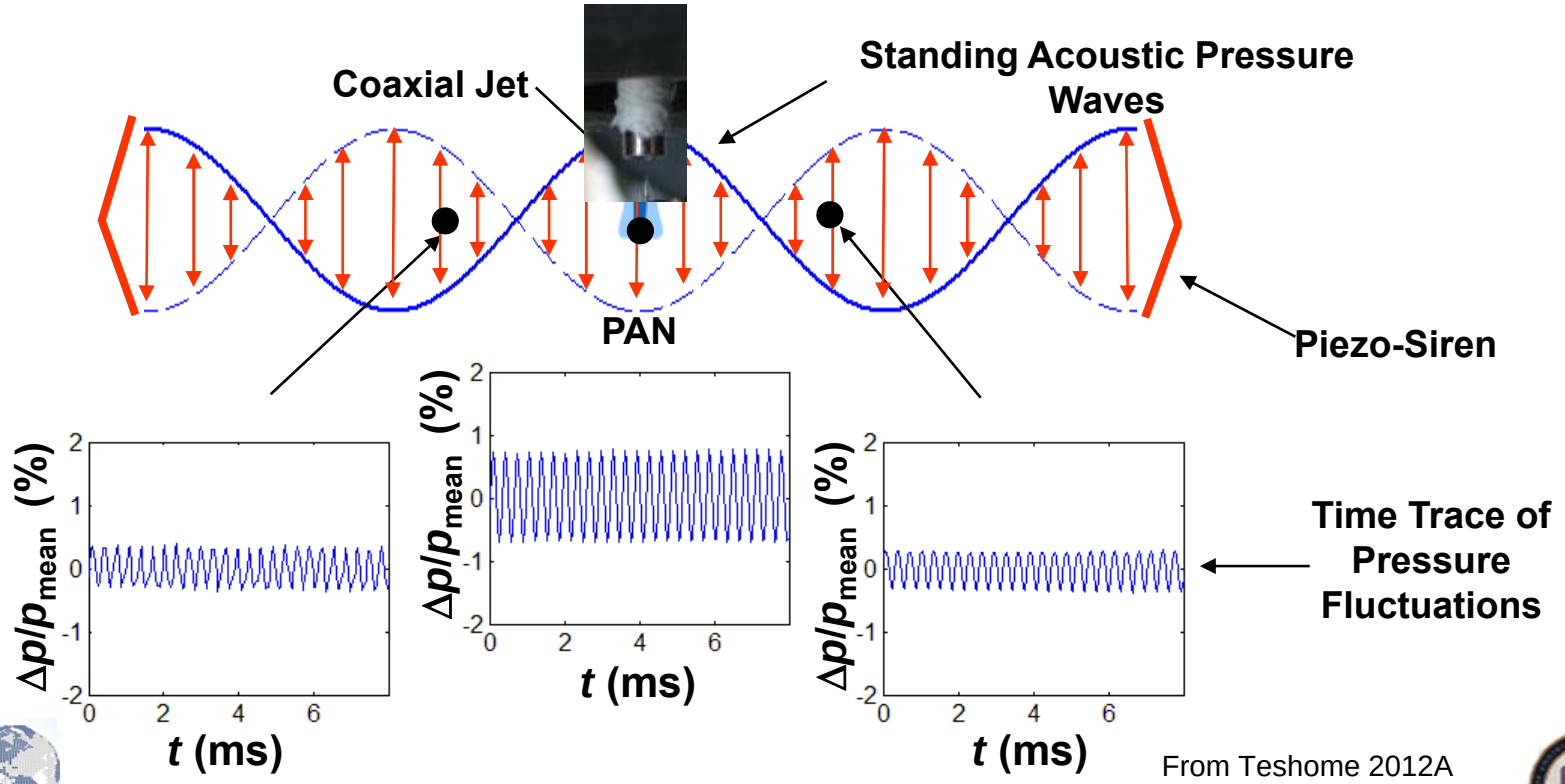

From Teshome 2012A

Proper orthogonal decomposition

• Proper Orthogonal Decomposition (POD was used for extracting dominant dynamical processes embedded in high-speed images.

• A time-resolved set of images $A(x,t)$ can be represented as a linear combination of orthonormal basis functions ϕ_k (aka proper orthogonal modes)[1,2,3] :

$$A(x,t) = \sum_{k=1}^{M} a_k(t)\phi_k(x)$$

where $a_k(t)$ are time dependent orthonormal amplitude coefficients and M is the number of modes

• Main idea: POD modal amplitudes capture the maximum possible "energy" in an average sense[4], i.e.,

$$\sum_k \langle a_k(t)a_k(t)\rangle \geq \sum_k \langle b_k(t)b_k(t)\rangle$$

where $b_k(t)$ are the temporal coefficients of a decomposition with respect to an arbitrary orthonormal basis ψ_k.

[1] **Chatterjee, A**. *Current Science*, Vol. 78, No. 7 (2000)
[2] **Arienti, M, and Soteriou, M.C.**. Phys. Fluids 21, 112104 (2009)
[3] **Berkooz, G., Holmes, P., and Lumley, J.L.**. *Annu. Rev. Fluid Mech.* 25. 539 (1993)

Construction of data set

• First, form a row vector consisting of all pixel intensity values of each snapshot image (with resolution of *n* rows by *m* columns) in order of increasing columns, then increasing rows

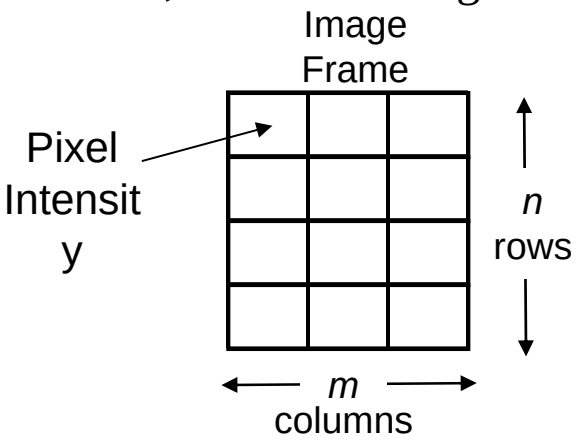

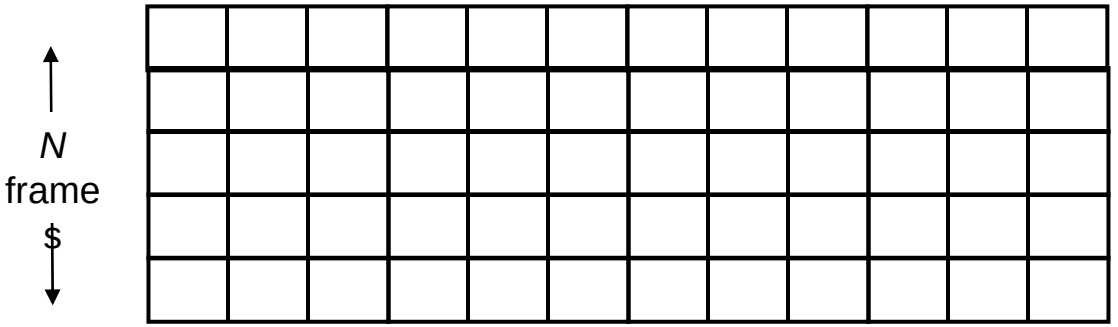

• Then, combine all such row vectors for *N* sequences of image frames resulting in a matrix **A** consisting of *N* rows by $P = n \times m$ columns of intensity values.

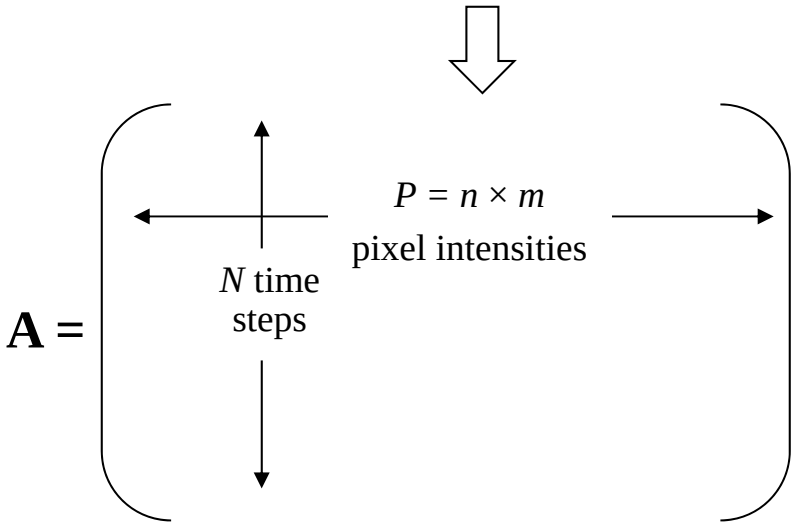

From Teshome 2012A

Orthogonal decomposition technique

- Eigenvalue decomposition or singular value decomposition (SVD) can be used
- SVD preferred since
  1. Applicable to non-square matrices (most likely the case)
  2. Decomposition matrices are orthogonal
  3. Subroutine readily available in MATLAB®
     - Subtracted temporal mean of $\mathbf{A} \Rightarrow$ matrix of intensity fluctuations $\tilde{\mathbf{A}}$
     - Applied SVD

$$\Rightarrow \tilde{\mathbf{A}} = \mathbf{U}\mathbf{S}\mathbf{V}^{\mathrm{T}} = \mathbf{Q}\mathbf{V}^{\mathrm{T}}$$

$N \times N$
Orthogonal Matrix of Left Singular Column Vectors of $\tilde{\mathbf{A}}$

$N \times N$
Diagonal Matrix of Singular Values

$N \times P$
Orthogonal Matrix of Right Singular Column Vectors of $\tilde{\mathbf{A}} \Leftrightarrow$ proper orthogonal modes (POM)

Columns of $\mathbf{Q} \sim a_k(t)$ contain temporal information

Columns of $\mathbf{V} \sim \phi_k(x)$ contain spatial information

From Teshome 2012A

Results – LAR-thin, *Pr* = 0.44, *J* = 5.2

LAR-thin

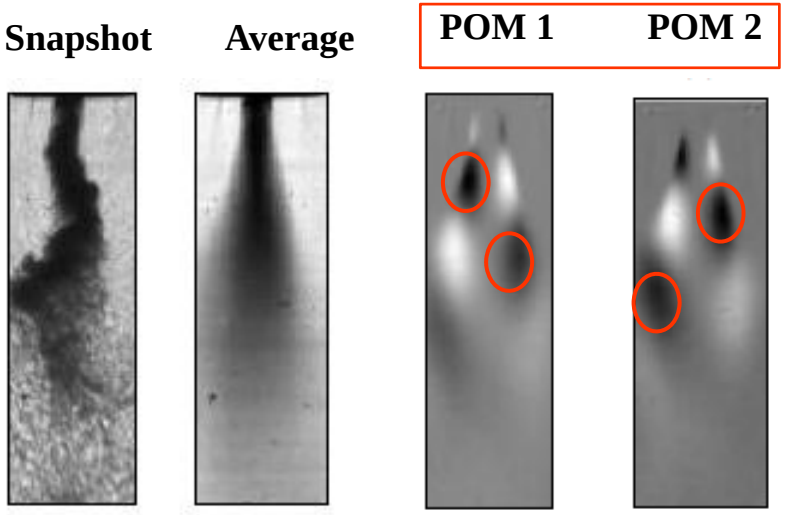

Amplitude information contained in singular values

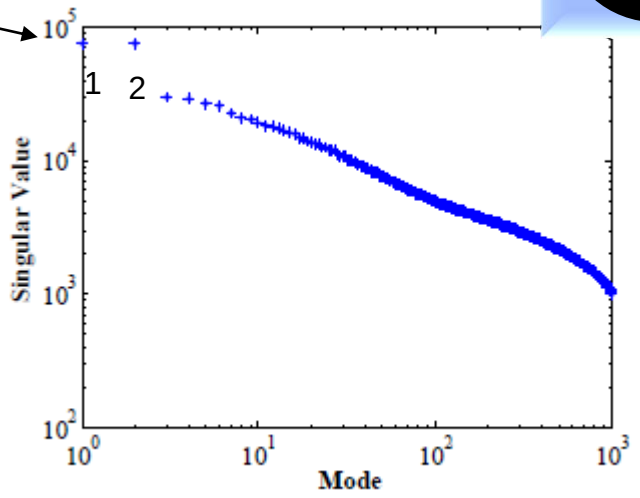

Antisymmetric Structures Identified with Characteristic Frequencies

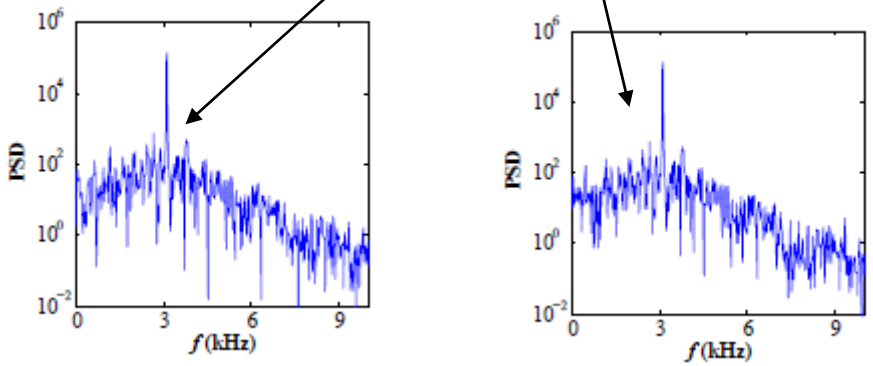

Power Spectral Densities (PSD) of Temporal Coefficients of POMs 1 and 2

From Teshome 2012A

Cross-Power Spectral Density (CPSD)

LAR-thin

- **CPSD yields the FFT of the cross-correlation of the temporal coefficients***

$$\mathrm{CPSD} = \sum_{k=0}^{N-1} \frac{\mathrm{cov}(a_x, a_y)}{\sigma_{a_x}\sigma_{a_y}} e^{-i\omega k}$$

- Magnitude and phase plots used to determine existence of propagating structures

LAR, *Pr* = 0.44, *J* = 5.2

PAN
(f_F = 3.12 kHz)

Baseline Spectrum Completely Removed in PAN Forced Spectrum

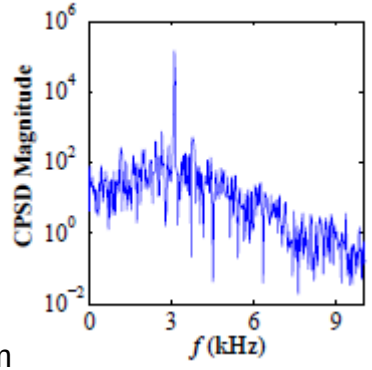

-90° Phase Difference Confirmed Downstream Propagating Flow Structures

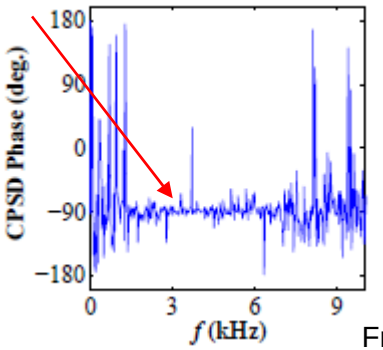

***Arienti, M, and Soteriou, M.C..** Phys. Fluids 21, 112104 (2009)

From Teshome 2012A

Results – LAR-thin Pr=0.44

- **Antisymmetric flow structures indicated helical type flow instabilities for all *J***

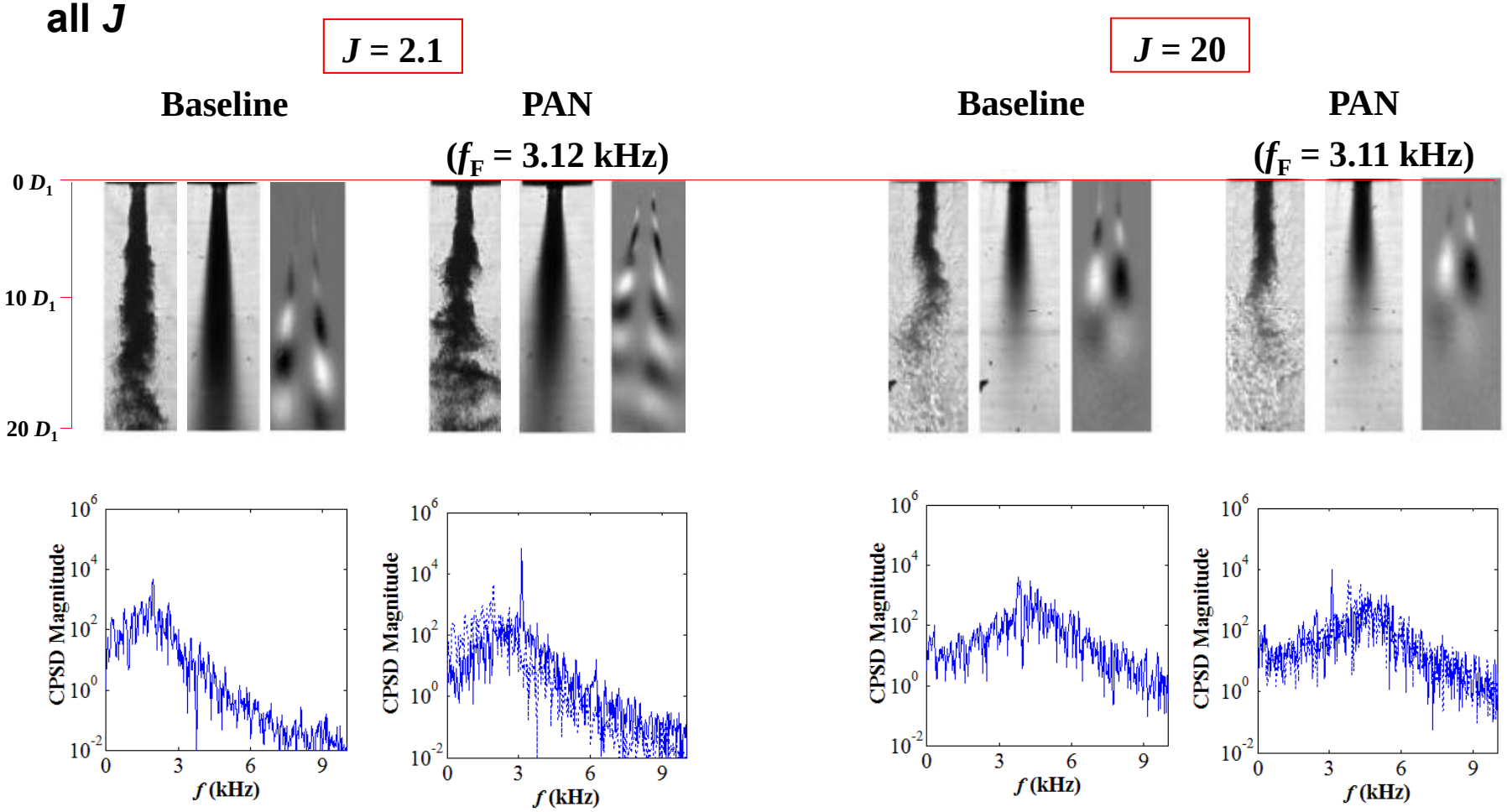

Geometry with least efficient mixing – less responsive to acoustics at high J

Results – SAR-thin Pr=0.44

SAR-thin

- Helical type flow instabilities became more well-defined with increasing *J*

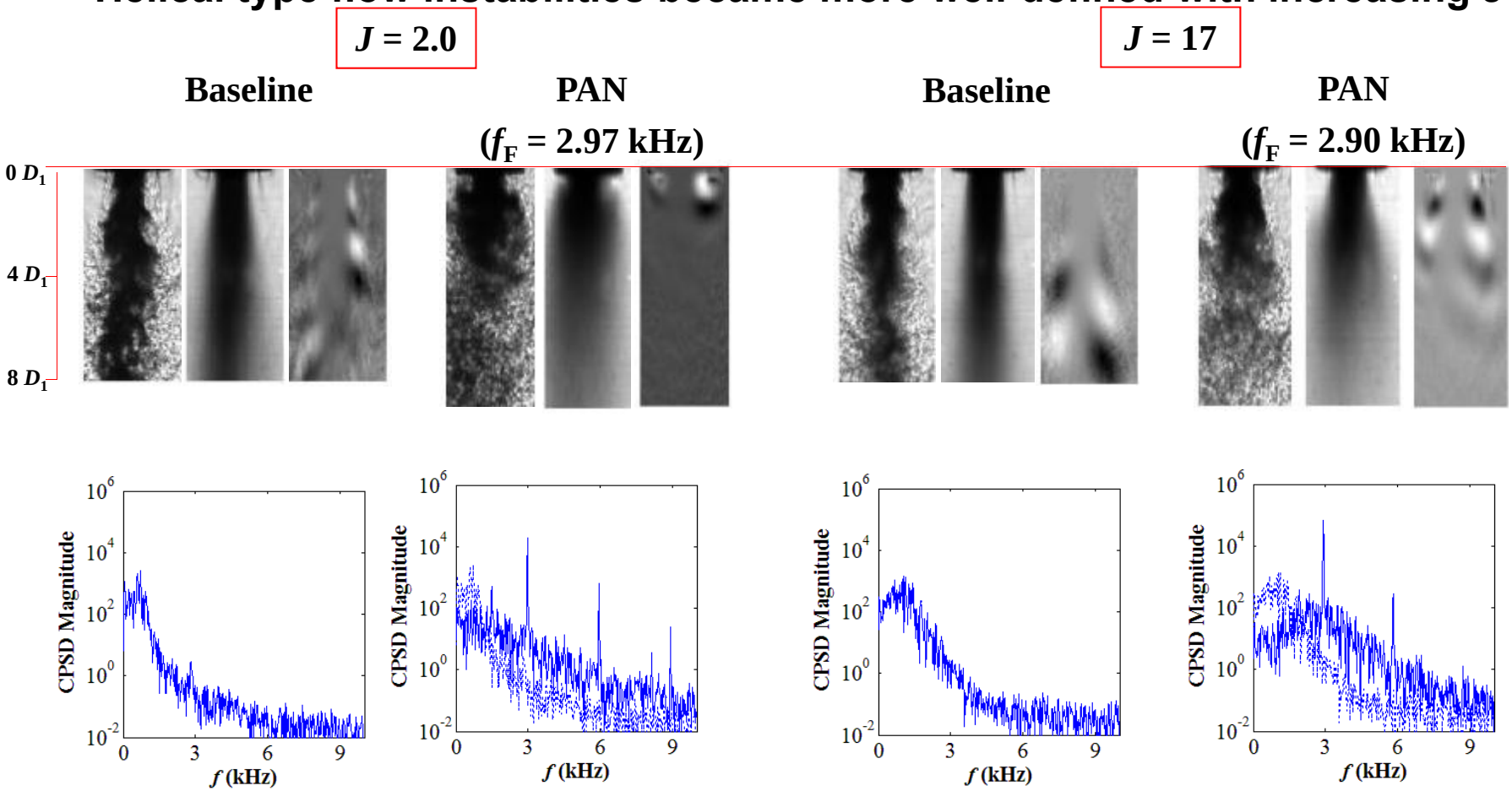

From Teshome 2012B

Results – SAR-thick, Pr=0.44

- **Helical type flow instabilities became more well-defined with increasing *J***

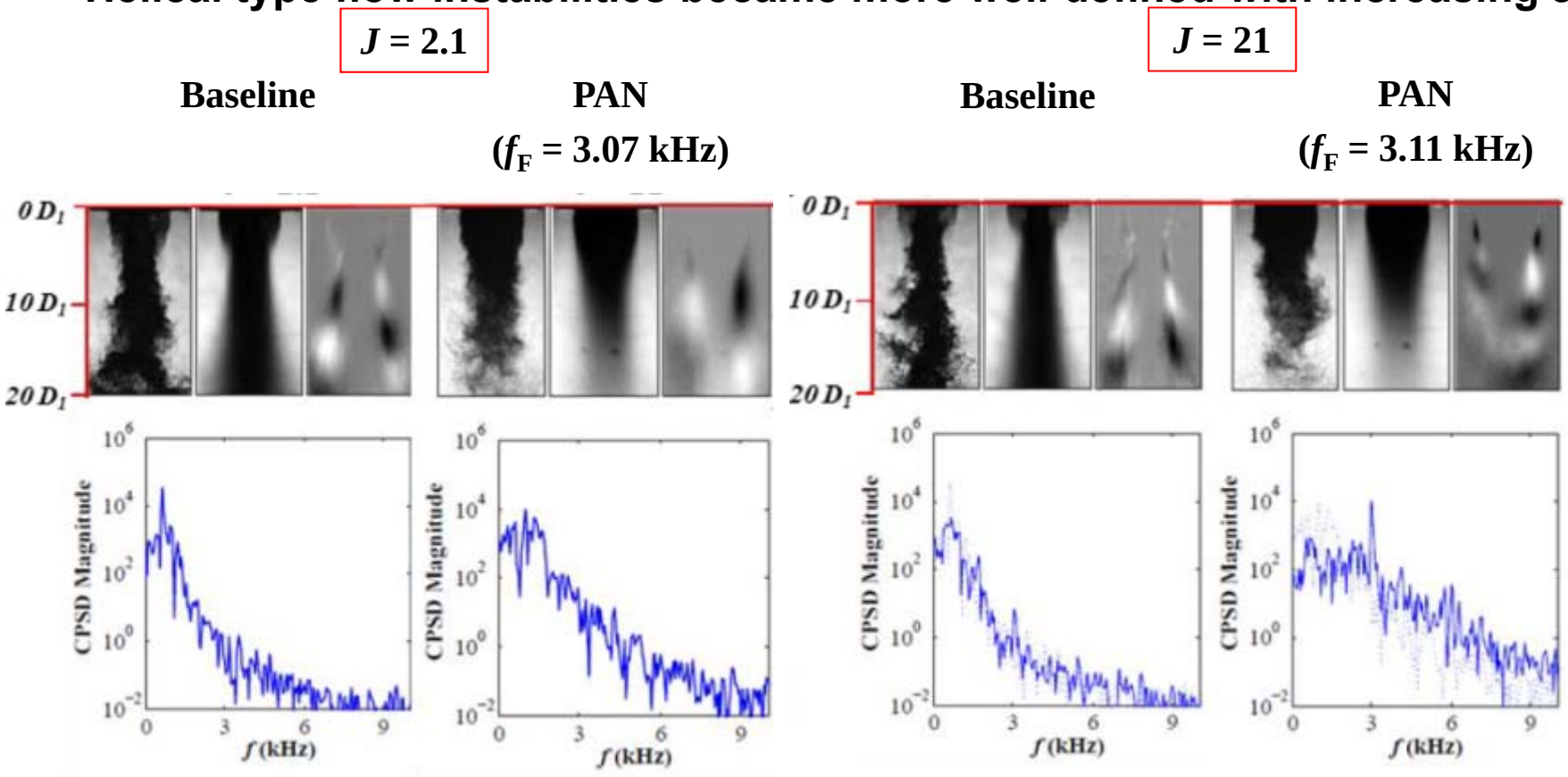

Geometry with most efficient mixing – more responsive to acoustics at high J

From Teshome 2012B

Collaboration with Caltech

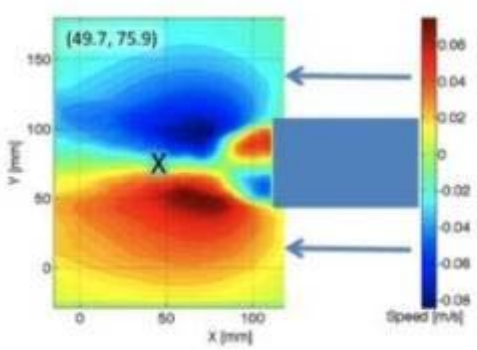

VR=1

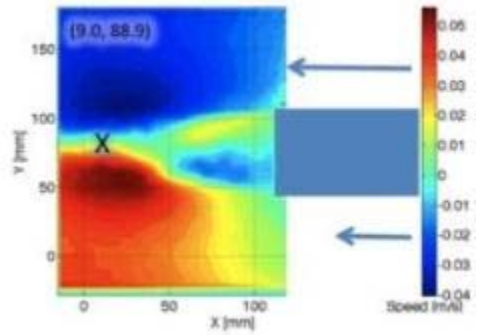

VR=0.55

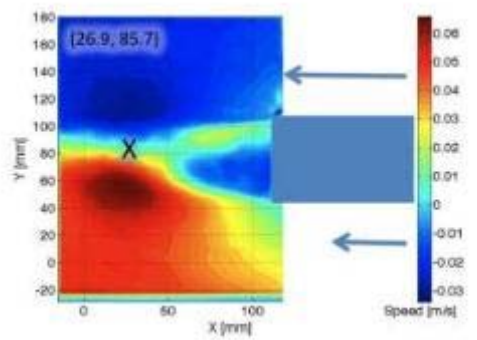

VR=0.33

- **Simplification of axisymmetric coaxial jets to a 2D setup**
- **Investigated effect of velocity ratio on St number on a water tunnel with PIV**

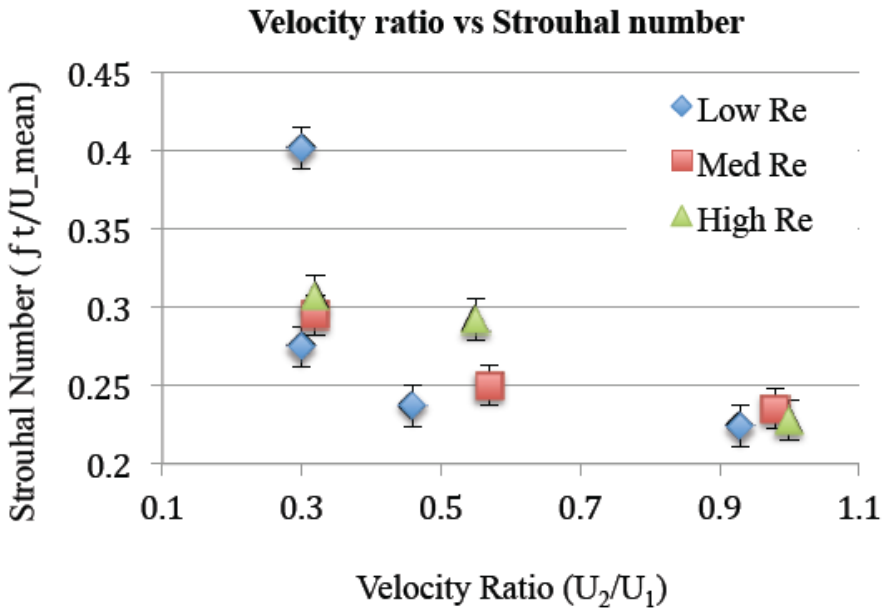

Differences in recirculation zone evident as VR decreases -- St decreases with VR

From: Split Stream Flow Past a Blunt Trailing Edge with Application to Combustion Instabilities, V. Tian, B. McKeon, I. Leyva, AIAA 2012-3807

Collaboration with Ecole Centrale Paris: comparison between CFD and experiments for shear coaxial jets

Velocity Fields for Different J values

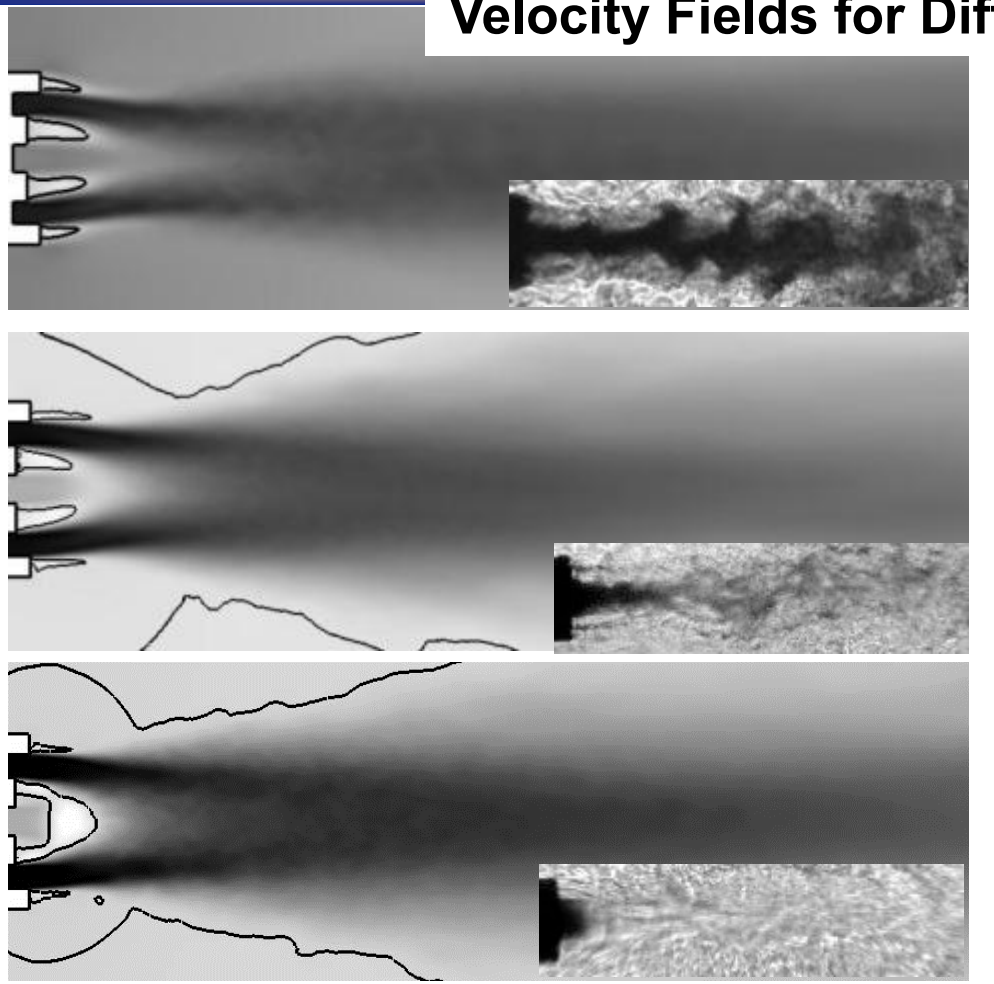

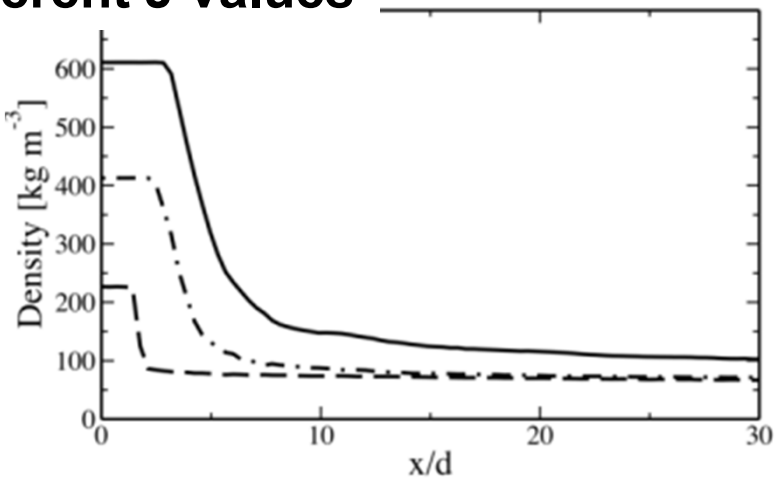

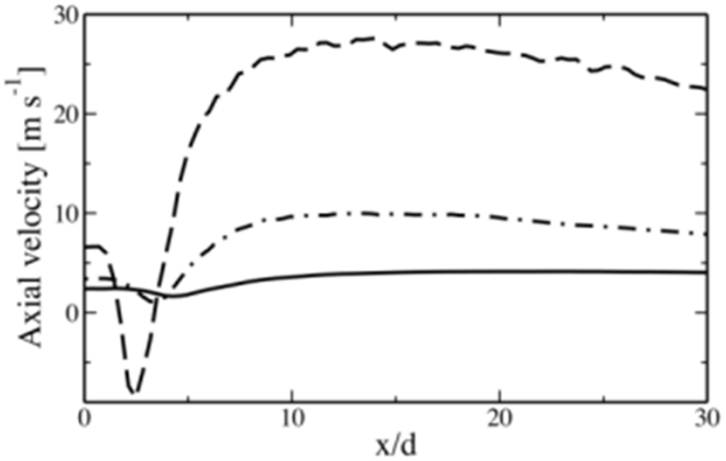

Longitudinal slice of axial velocity. White: minimum; black: maximum. Dark line indicates iso-contour of zero axial velocity. Top: J = 1.1; middle: J = 3.0; bottom: J = 9.3.

Top: centerline profile of density; bottom: centerline profile of velocity. Dark line: J = 1.1; dash point line: J = 3.0; dashed line: J = 9.3.

From Experiments and numerical simulation of mixing under supercritical conditions, T. Schmitt, J. Rodriguez, I. A. Leyva, and S. Candel, Physics of Fluids 24, 2012

Fundamental frequencies for baseline conditions

Case "N6" (*J=3.05*) *Density distribution (white: 60 kg/m³; black: 410 kg /m³; logarithmic scale).*

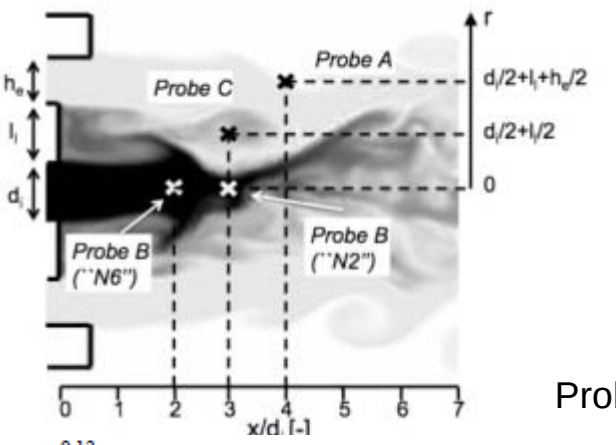

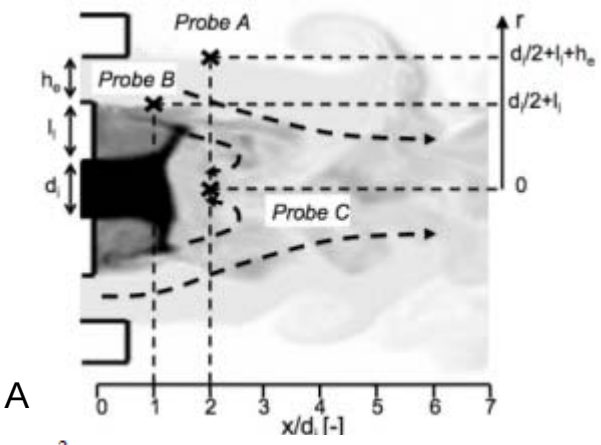

Probe A

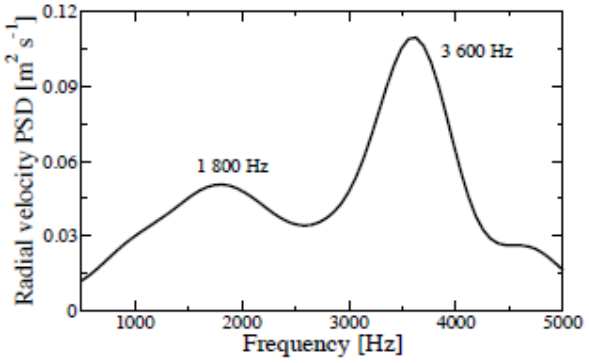

(b)

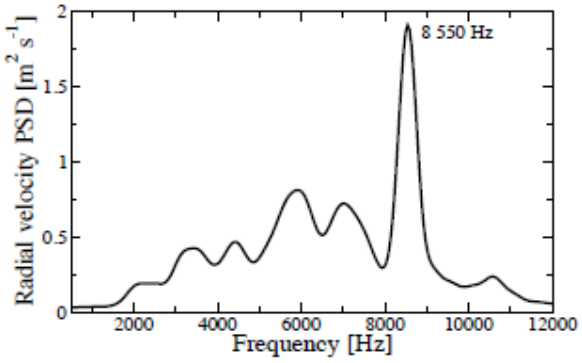

Case "N8" (*J = 9.3*) *Density distribution (white: 60 kg/m³; black: maximum ; logarithmic scale).*

OUTER JET

J=1.05

R=2.48

OUTER JET

J=3.05

R=4.18

Case	$St^e = h_e f/U_{oj}$ (probe A)	$St^i = d_i f/U_{ij}$ (probe B)	$St^l = l_l f/U_{oj}$ (probe C)
N2	0.25	0.34	0.15
N6	0.25	0.26	0.14

Found relevant St numbers for our configurations

Conclusions 1/2

- Research on shear coaxial jets goes back to 60s
- First researchers focused on the development of the jets for different variables: R, geometry
  - Defined the different mixing regions in a shear coaxial injector – inner and outer potential cores
  - Made a lot of very rich visualizations and measurements
  - Found functional relations between R and the potential core
- A lot of previous work investigates the relevant St for the inner and outer jets and what happens when jets are modulated close to their preferred modes
- In the last ten years a lot of progress has been made on LES and DNS to better understand the mixing processes in shear coaxial jets
- AFRL has published results on four geometries with the primary goal of understanding mixing in unforced and acoustically driven shear coaxial jets
  - The mixing process is measured qualitatively by the dark core which is related to the potential core for both unforced and driven conditions

Conclusions 2/2

- J is not the only parameter to characterize mixing in shear coaxial jets - area ratio, inner jet post thickness and density also matter
- Found functional correlations for dark core lengths
- Proper orthogonal decomposition of high-speed image intensity fluctuation data revealed key spatial and temporal characteristics of flow structures
- Based on four geometries, mixing is enhanced with increasing J and t/D1 but less efficient with increasing Ao/Ai
- Helical instabilities were observed for Pr=0.44 for LAR-thin, SAR-thick, and SAR-thin geometries at large J for baseline conditions
- Geometry plays a role for the response of the jet to acoustics, at Pr=0.44 PAN:
  - LAR-thin: The flow became less sensitive to applied PAN forcing with increasing J
  - SAR-thin: Flow responds to forcing acoustic frequency at all J
  - SAR-thick: Recirculation zone dampens the effect of PAN forcing at lower J, but at higher J (>10) measurable effect

BACKUP MATERIAL

Baseline flows: LAR-thin injector

$P_r = 0.44$

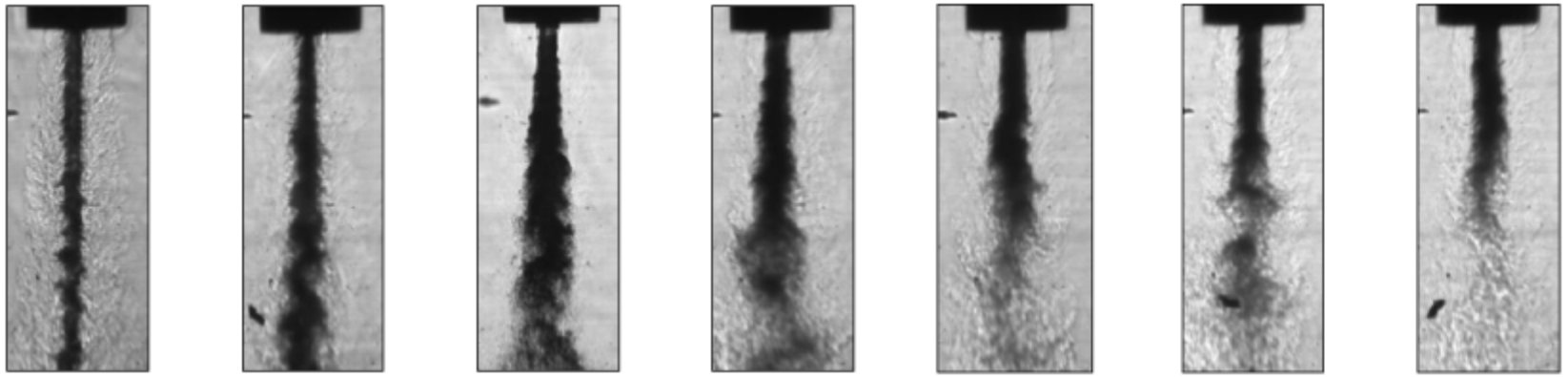

$J = 0.1$ 0.5 2.1 5.2 11 14 20

$P_r = 1.05$

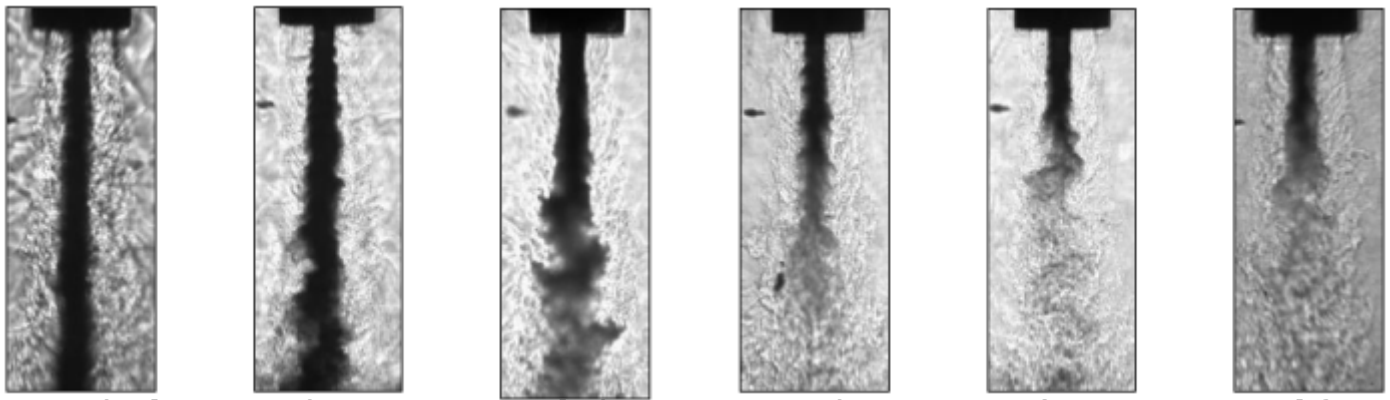

$J = 0.1$ 0.5 1.9 5.0 8.5 12

From Teshome 2012A

Baseline flows: SAR-thick injector

$P_r = 0.44$

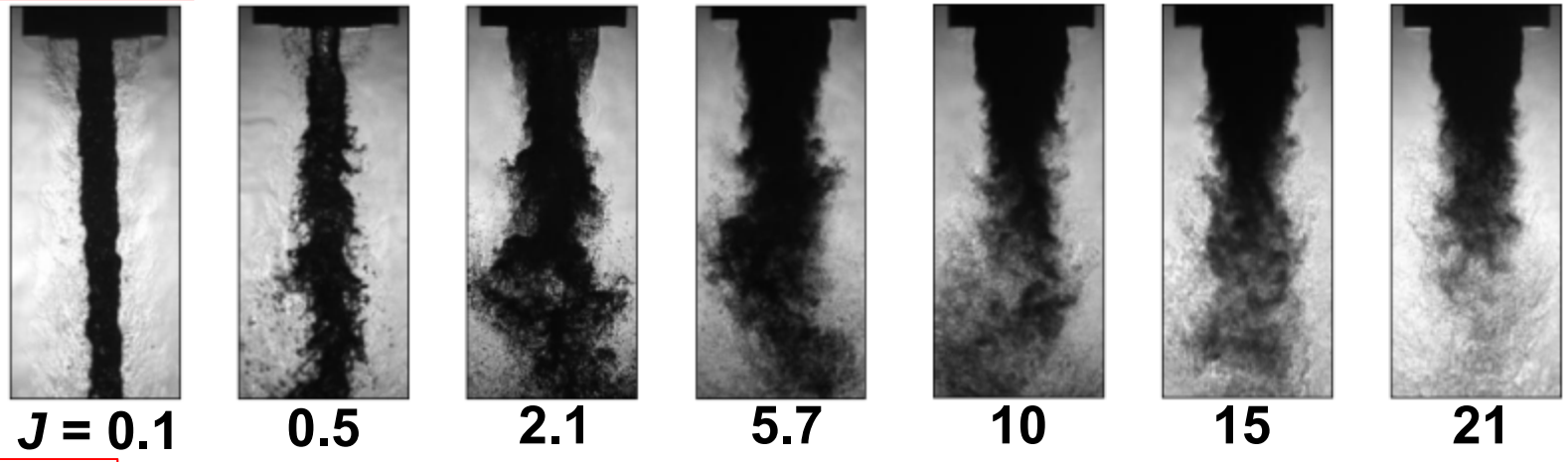

$J = 0.1$ 0.5 2.1 5.7 10 15 21

$P_r = 1.05$

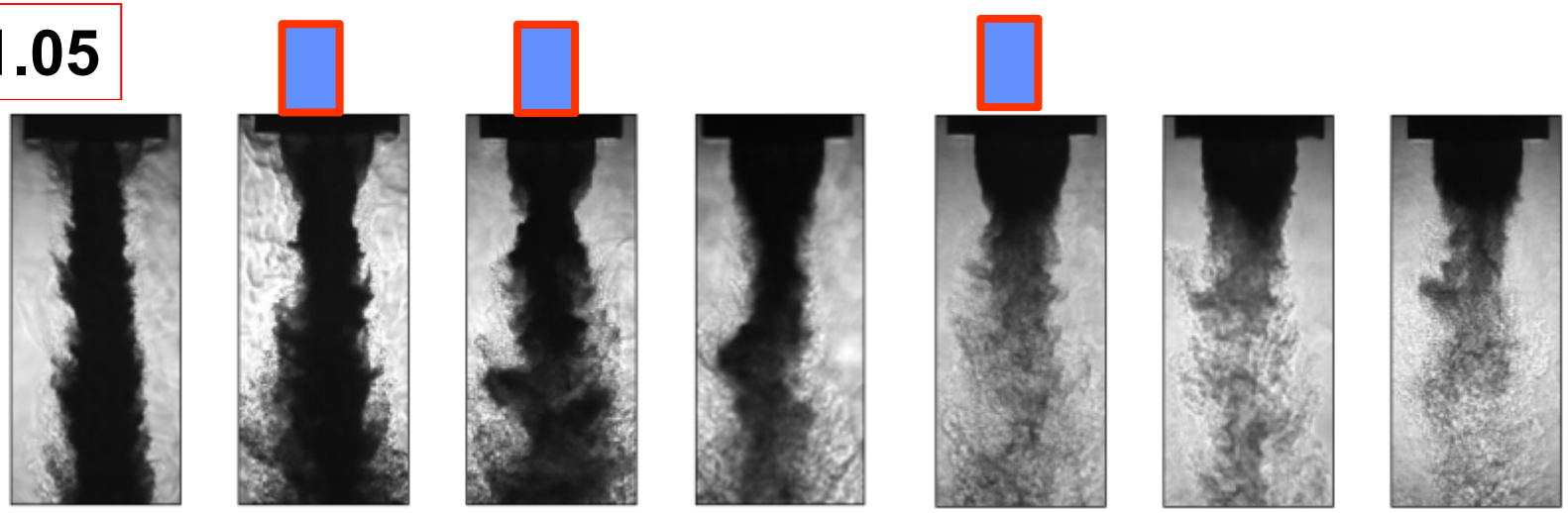

$J = 0.1$ 0.5 2.1 5.2 9.2 14 21

From Teshome 2012A

Image interpretation key

Baseline:
Acoustics
off

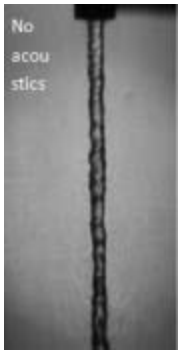

0^{o}
Acoustics on
PAN, VN
"Pressure coupled"

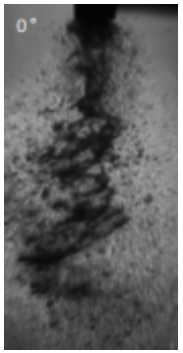

180^{o}
PN, VAN
Largest difference
expected from 0^{o}
"Velocity coupled"

pressure = fixed

$J\ (\rho_o u_o^2/\rho_i u_i^2)$ = fixed

PN – pressure node - Min
PAN – pressure antinode - Max
VN – velocity node
VAN – velocity antinode

From J. I. Rodriguez. Acoustic Excitation of Liquid Fuel Droplets and Coaxial Jets. Ph.D. dissertation, UCLA, 2009.

Matrix Decomposition

- **Eigenvalue decomposition or singular value decomposition (SVD) can be used**
- **SVD Subroutine readily available in MATLAB®**
- **Prior to matrix decomposition, the temporal mean of A was subtracted resulting in a matrix of intensity fluctuations Ã, i.e.,**

$$\tilde{A}_{ij} = A_{ij} - \frac{1}{N}\sum_{i} A_{ij} \qquad \text{for } i = 1\ldots N,\ j = 1\ldots M$$

- **Application of SVD on Ã gives two orthogonal matrices U (NxN) and V (MxM), and a diagonal matrix S (NxM) of singular values in increasing order of magnitude**

$$\tilde{A} = USV^{T} = QV^{T}$$

- **Thus, a time-resolved set of images intensity fluctuations Ã(x,t) can be represented as a linear combination of orthonormal basis functions ϕ_k such that**

$$\tilde{A}(x,t) = \sum_{k=1}^{M} a_k(t)\phi_k(x)$$

where $a_k(t)$ are time dependent orthonormal amplitude coefficients and ϕ_k(x) are the proper orthogonal modes of Ã.

- **Equivalence: columns of Q ~ $a_k(t)$, columns of V ~ ϕ_k(x)**

Collaboration with ECP: grid and mesh

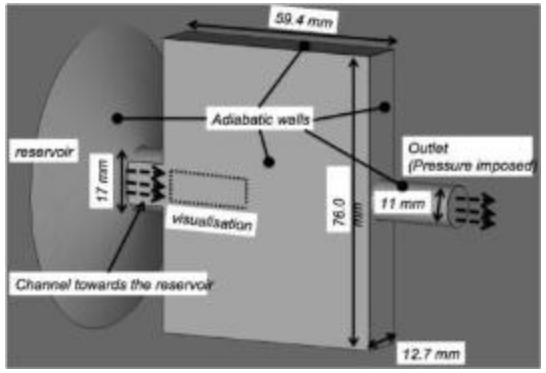

3D visualization of reservoir

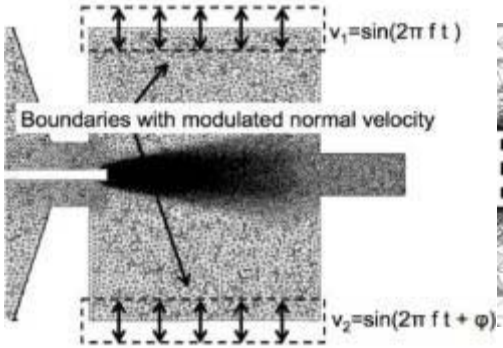

Longitudinal cut of domain with the BC's

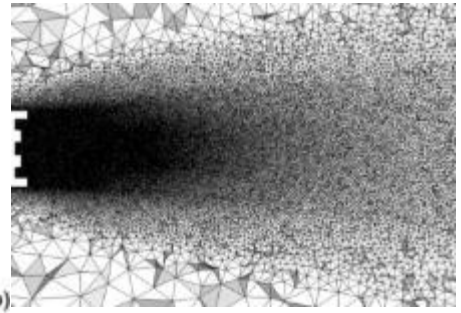

Mesh detail near the injector

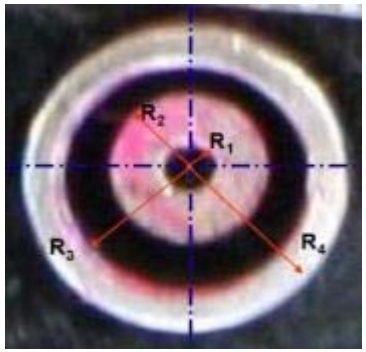

Experimental Injector

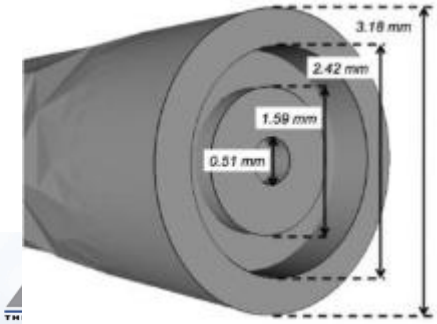

CFD Injector

- **Solver: AVBP – state of the art LES code**
  - **With real fluid properties to tackle supercritical fluids**
- **Mesh: 2 100 000 nodes/10 000 000 tetrahedra**
  - **Highly refined near the injector (0.032 mm on a distance of 10 inner jet diameters)**
- **CPU hours on Europe SuperComputer Center: 100,000**

From Experiments and numerical simulation of mixing under supercritical conditions, T. Schmitt, J. Rodriguez, I. A. Leyva, and S. Candel, Physics of Fluids 24, 2012

Acoustic forcing results

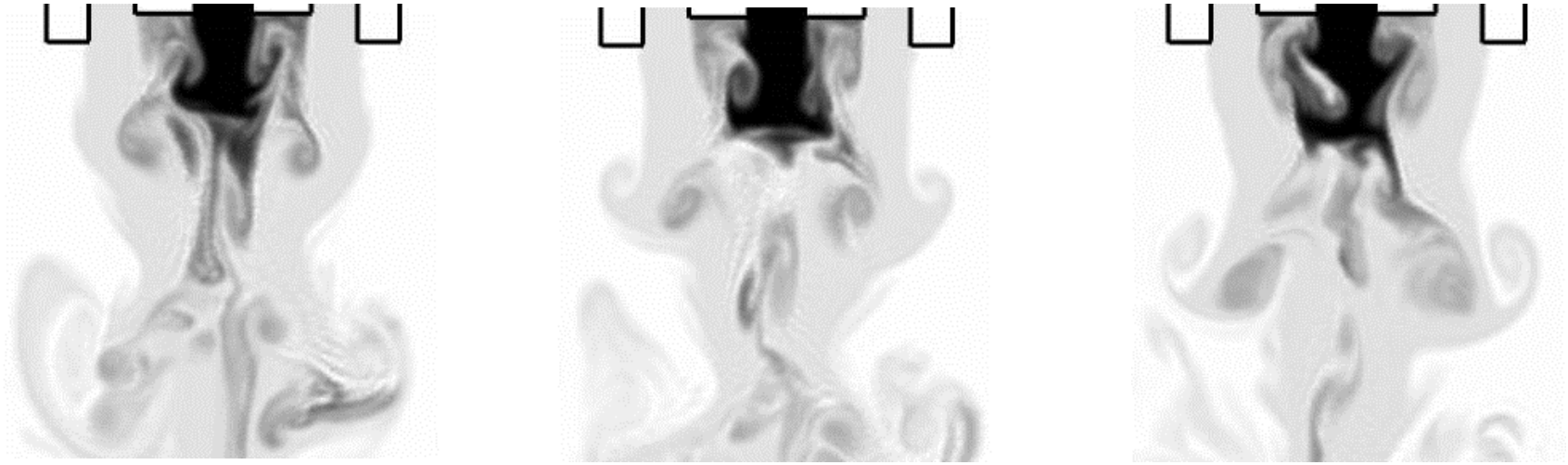

Instantaneous images of the simulation of an acoustic case with the injector at a pressure antinode for a J = 3.0

From Experiments and numerical simulation of mixing under supercritical conditions, T. Schmitt, J. Rodriguez, I. A. Leyva, and S. Candel· Physics of Fluids 24, 2012

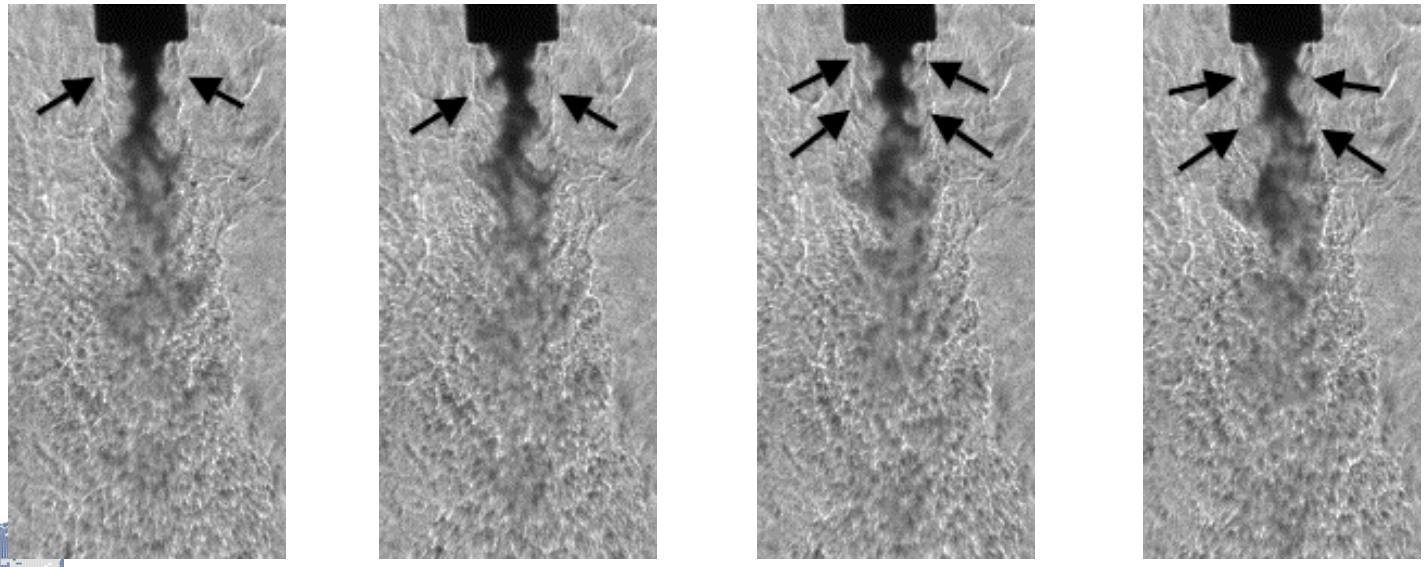

Instantaneous images of an experimental acoustic case with the injector at a pressure antinode for a J = 2.9

Subcritical low J

$P_{chamber}$ = 1.5 MPa (Pr = 0.44)

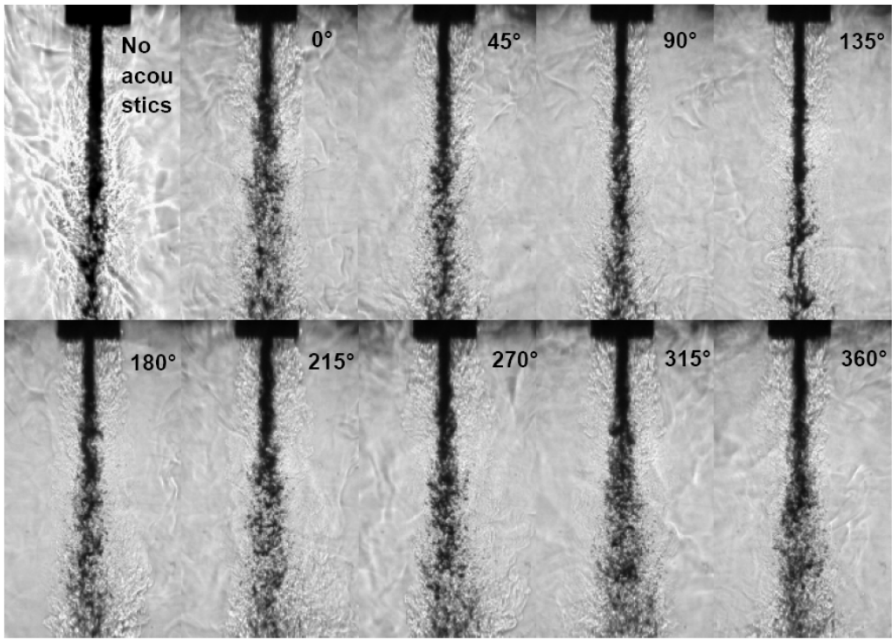

J = 0.17

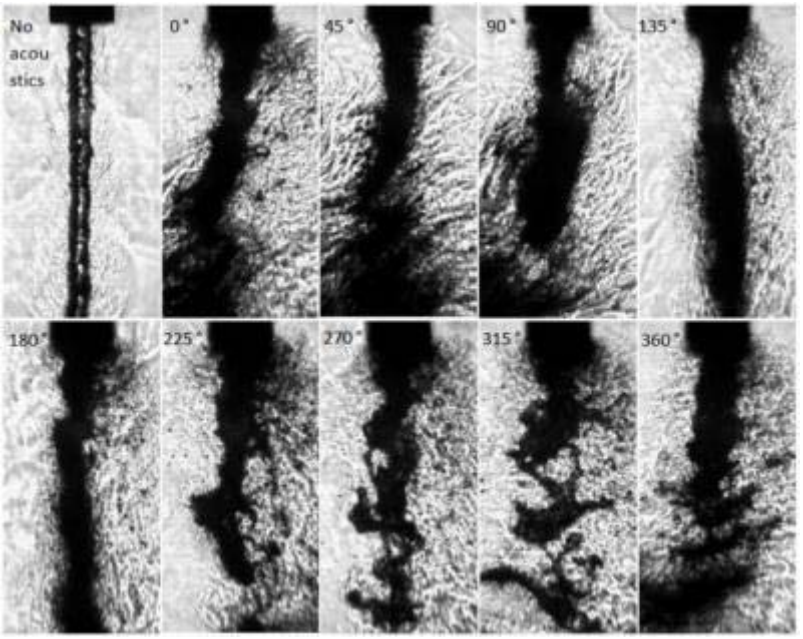

J = 0.089 with thin inner post injector

Negligible effect vs. violent destruction of the jet

From J. I. Rodriguez. Acoustic Excitation of Liquid Fuel Droplets and Coaxial Jets. Ph.D. dissertation, UCLA, 2009.

Subcritical Moderate J

$P_{chamber}$ = 1.5 MPa (Pr = 0.44)

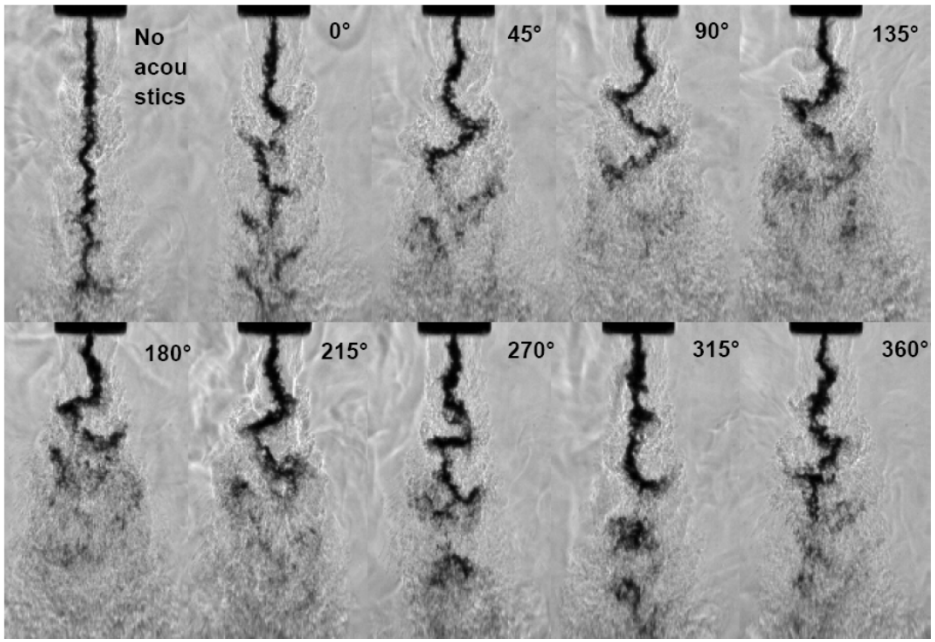

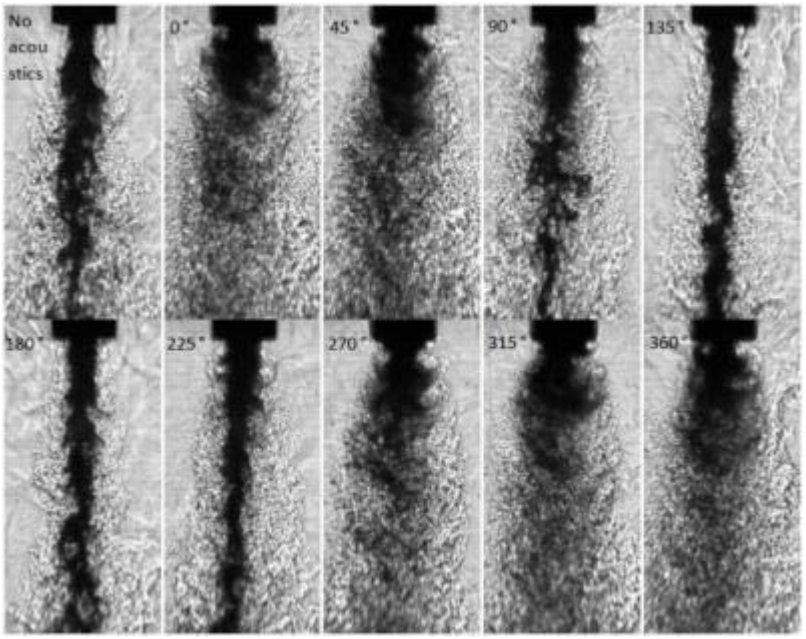

J = 2.6 with thick inner post injector

J = 2.0 with thin inner post injector

Bending vs. vortical structures with fine atomization

From J. I. Rodriguez. Acoustic Excitation of Liquid Fuel Droplets and Coaxial Jets. Ph.D. dissertation, UCLA, 2009.

Subcritical large J

$P_{chamber}$ = 1.5 MPa (Pr = 0.44)

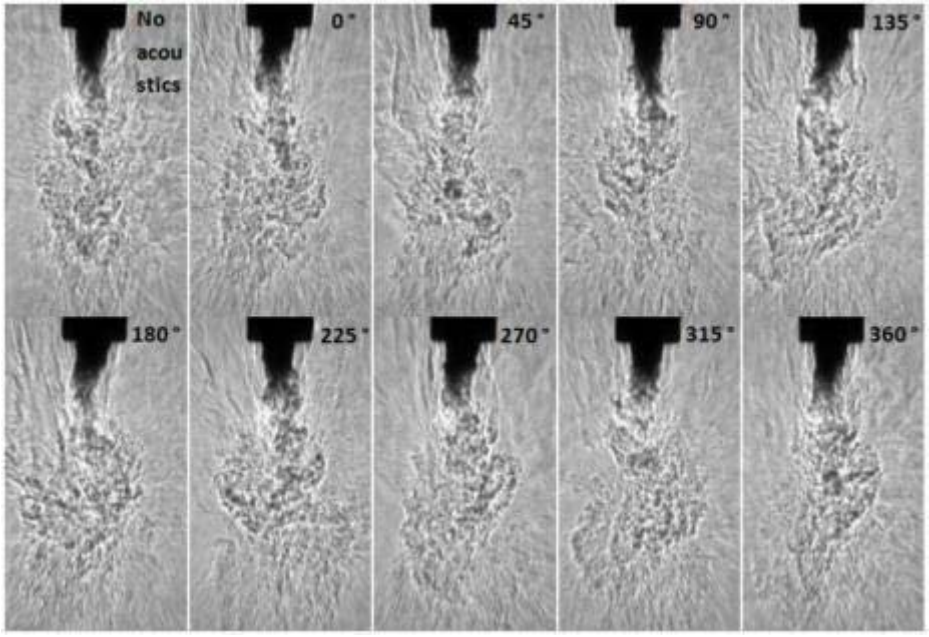

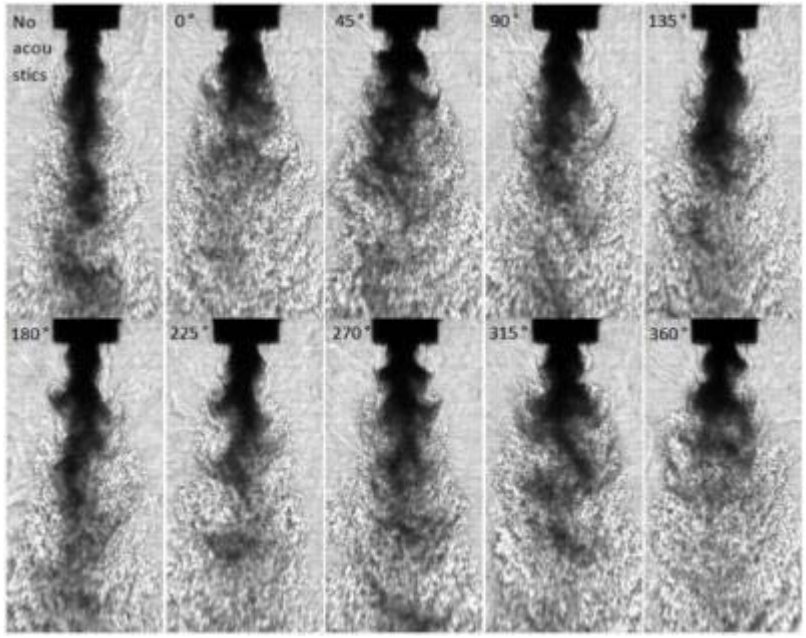

J = 23 with thick inner post injector

J = 18 with thin inner post injector

Two different mixing mechanisms for similar large J values

From J. I. Rodriguez. Acoustic Excitation of Liquid Fuel Droplets and Coaxial Jets. Ph.D. dissertation, UCLA, 2009.

Nearcritical large J

$P_{chamber}$ = 3.6 MPa (Pr = 1.1)

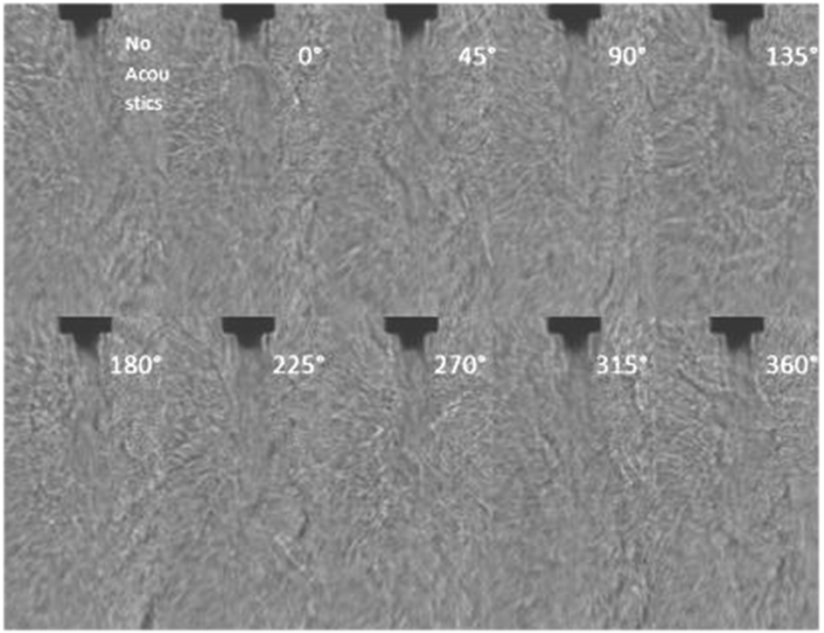

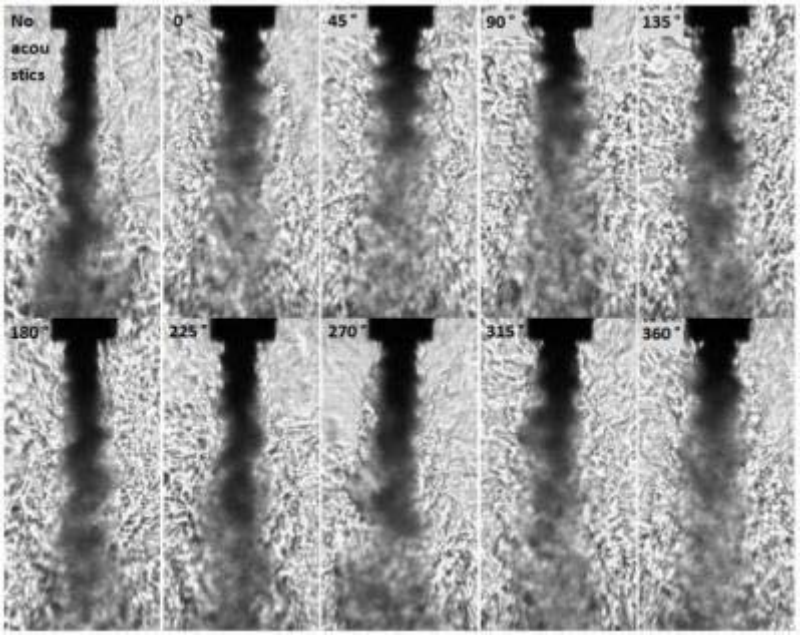

J = 9.3 with thick inner post injector

J = 9.4 with thin inner post injector

Longer dark core lengths and hence visible effect of acoustics for thin inner post geometry

From J. I. Rodriguez. Acoustic Excitation of Liquid Fuel Droplets and Coaxial Jets. Ph.D. dissertation, UCLA, 2009.

Supercritical moderate J

$P_{chamber}$ = 5.0 MPa (Pr = 1.5)

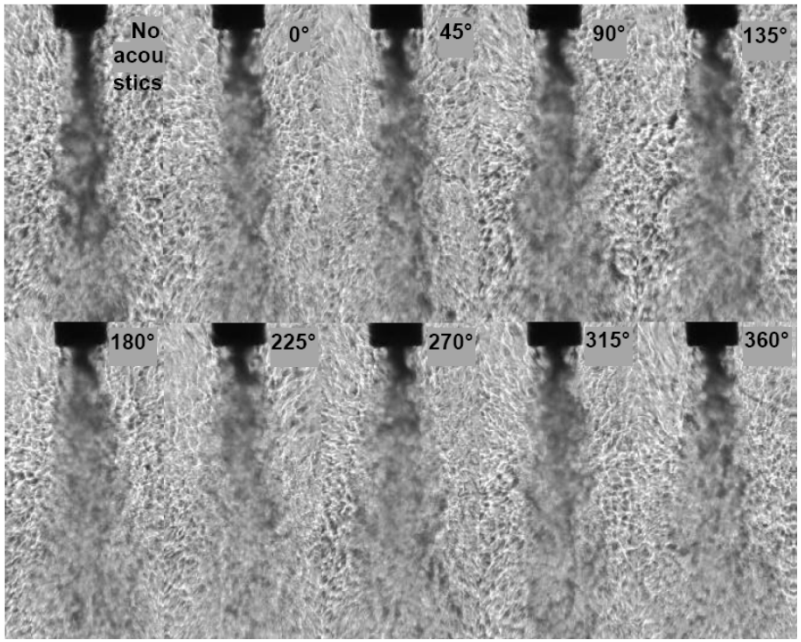

J = 2.4 with thick inner post injector

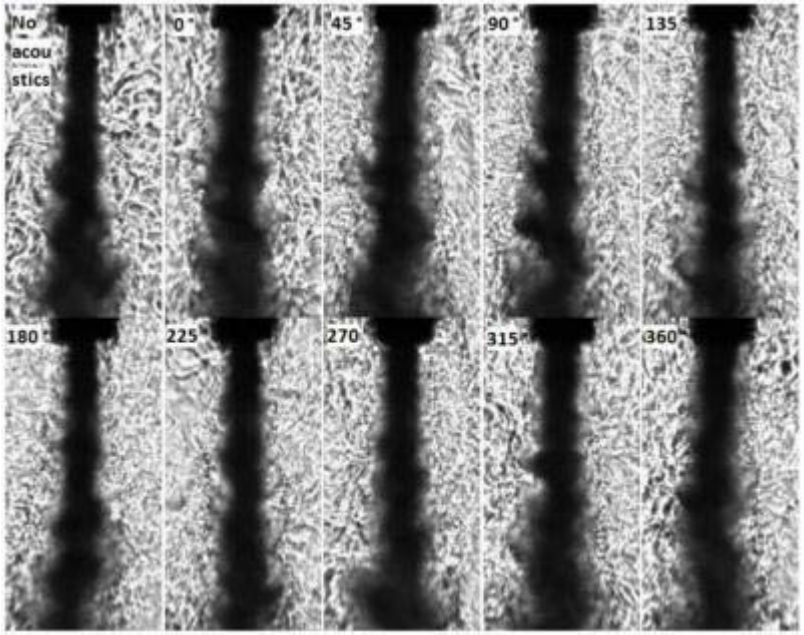

J = 2.6 with thin inner post injector

Large dark core lengths for the thin post geometry prevent us from observing acoustic effects, if any

From J. I. Rodriguez. Acoustic Excitation of Liquid Fuel Droplets and Coaxial Jets. Ph.D. dissertation, UCLA, 2009.

LAR-thick

	$T_{chamber}$ (K)	$\rho_{chamber}$ (kg/m^3)	$P_{chamber}$ (MPa)	T_{outer} (K)	$\dot{m}_{outer}$ (mg/s)	ρ_{outer} (kg/m^3)	u_{outer} (m/s)	Re_{outer} (10^4)	T_{inner} (K)	$\dot{m}_{inner}$ (mg/s)	ρ_{inner} (kg/m^3)	u_{inner} (m/s)	Re_{inner} (10^4)	L/D_1 (baseline)	Freq. (kHz)	$P'_{RMS\ max}$ (kPa)	VR	J
SUB																		
sub1	233	22.0	1.50	191	310	27.6	4.30	0.768	109	279	630	2.2	1.2	26.2	2.98	21.5	2.0	0.17
sub2	231	22.2	1.50	183	790	28.8	11.0	2.02	109	283	630	2.2	1.2	17.1	3.06	20.1	4.8	1.0
sub3	226	21.9	1.45	183	1230	27.8	16.9	3.16	109	284	630	2.2	1.2	16.6	3.06	17.8	7.6	2.6
sub4	226	22.9	1.51	185	1560	28.7	20.9	3.96	109	279	630	2.2	1.2	15.2	2.96	15.7	9.5	4.2
sub5	210	24.9	1.50	182	2400	29.3	31.3	6.18	109	279	630	2.2	1.2	8.40	3.01	16.9	14	9.6
sub6	216	24.1	1.50	191	3640	27.7	50.3	9.02	109	279	630	2.2	1.2	5.63	3.02	16.3	23	23
NEAR																		
near1	223	56.6	3.58	180	1060	75.4	5.38	2.58	123	290	520	2.8	2.0	24.4	3.08	9.04	2.0	0.55
near2	207	62.0	3.57	152	1570	101	5.95	4.16	117	289	590	2.4	1.5	15.5	3.04	10.8	2.5	1.0
near3	228	55.1	3.58	185	1590	72.4	8.40	3.80	126	293	440	3.3	2.5	14.6	3.00	11.8	2.6	1.1
near4	223	56.1	3.55	184	2170	72.3	11.5	5.21	127	294	360	4.0	3.4	12.1	3.01	11.4	2.8	1.6
near5	230	54.2	3.56	199	2120	65.1	12.5	4.84	126	292	440	3.3	2.5	12.9	3.03	12.1	3.8	2.1
near6	229	54.5	3.56	183	2690	73.1	14.1	6.48	126	292	420	3.4	2.5	5.98	3.05	11.1	4.1	2.9
near7	219	57.6	3.56	194	3080	67.4	17.5	7.15	125	289	480	3.0	2.2	5.56	3.06	11.8	5.9	4.9
near8	213	59.6	3.56	192	6460	68.3	36.2	15.1	128	295	220	6.6	5.2	2.45	2.93	9.73	5.5	9.3
SUPER																		
super1	231	76.1	4.96	198	292	93.9	1.19	0.642	136	291	300	4.8	3.9	37.7	3.05	8.01	0.25	0.019
super2	231	76.1	4.96	193	997	97.7	3.90	2.22	130	292	460	3.1	2.4	26.7	3.01	10.2	1.2	0.33
super3	221	80.4	4.95	180	2050	109	7.19	4.72	128	291	490	2.9	2.1	19.2	3.01	10.7	2.5	1.3
super4	222	80.1	4.96	182	3110	107	11.1	7.13	134	288	360	3.9	3.3	10.2	3.05	10.1	2.8	2.4
super5	222	80.3	4.97	191	2820	99.5	10.8	6.32	131	293	440	3.3	2.6	9.02	3.09	12.5	3.3	2.5
super6	211	85.8	4.96	187	5820	103	21.6	13.2	132	286	410	3.4	2.7	3.04	3.05	10.7	6.3	9.9

From J. I. Rodriguez. I. Leyva, J. Graham, D. Talley, Mixing Enhancement of Liquid Rocket Engine Injector Flow, AIAA 2009-5143

SAR-thin

	$T_{chamber}$ (K)	$\rho_{chamber}$ (kg/m^3)	$P_{chamber}$ (MPa)	T_{outer} (K)	$\dot{m}_{outer}$ (mg/s)	ρ_{outer} (kg/m^3)	u_{outer} (m/s)	Re_{outer} (10^4)	T_{inner} (K)	$\dot{m}_{inner}$ (mg/s)	ρ_{inner} (kg/m^3)	u_{inner} (m/s)	Re_{inner} (10^4)	L/D_1 (baseline)	Freq. (kHz)	$P'_{RMS\ max}$ (kPa)	VR	J
SUB																		
subnew1	235	22	1.48	199	90	26	1.4	0.21	105	920	660	0.91	1.3	13+	3.01	8.86	1.5	0.089
subnew2	237	22	1.49	197	200	26	3.0	0.47	106	925	655	0.92	1.3	13+	2.96	14.0	3.3	0.43
subnew3	246	21	1.49	195	450	27	6.6	1.1	109	925	630	0.96	1.5	11+	2.97	12.1	6.9	2.0
subnew4	224	23	1.49	189	600	28	8.5	1.5	110	925	620	0.97	1.5	10.4	3.04	10.2	8.7	3.4
subnew5	217	24	1.49	184	750	29	10	1.9	110	925	620	0.97	1.5	9.29	3.02	11.5	11	5.2
subnew6	228	22	1.49	193	880	27	13	2.1	108	925	640	0.94	1.4	8.08	2.96	12.7	14	7.8
subnew7	222	23	1.49	194	1100	27	16	2.6	108	925	640	0.94	1.4	7.63	2.92	11.2	17	12
subnew8	217	24	1.48	201	1300	26	20	3.0	109	925	630	0.96	1.5	7.26	2.90	9.16	21	18
NEAR																		
nearnew1	228	55	3.56	213	330	60	2.2	0.70	109	925	650	0.93	1.3	14+	2.98	10.8	2.3	0.50
nearnew2	226	55	3.56	209	460	61	3.0	1.0	109	925	650	0.93	1.3	14+	3.06	9.17	3.2	0.97
nearnew3	230	54	3.58	198	730	66	4.3	1.6	108	925	655	0.92	1.3	13+	3.00	9.12	4.7	2.2
nearnew4	216	59	3.58	199	1030	65	6.3	2.3	109	925	650	0.93	1.3	13+	3.11	16.0	6.7	4.6
nearnew5	214	59	3.58	203	1460	63	9.2	3.2	109	925	650	0.93	1.3	7.01	3.07	15.0	9.9	9.4
nearnew6	215	59	3.56	207	2060	62	13	4.5	111	925	635	0.95	1.4	3.55	3.09	18.3	14	19
SUPER																		
supernew1	219	81	4.95	212	890	85	4.1	1.8	111	925	650	0.93	1.4	13+	3.11	17.0	4.4	2.6

From J. I. Rodriguez. I. Leyva, J. Graham, D. Talley, Mixing Enhancement of Liquid Rocket Engine Injector Flow, AIAA 2009-5143

Chronological progression (only coaxial results are summarized in what follows)

- Single jets, no coaxial flow
  - Davis et. al. (Ph.D. thesis) – single jets, no coaxial flow
- Coaxial jets
  - Davis et al. (Ph.D. thesis) – LAR thick
  - Leyva et.al. – LAR_thick
  - Rodriguez et. al. (Ph.D. thesis) – LAR_thick, SAR_thin
  - Graham et. al. – SAR_thin, two recesses
  - Teshome et. al. (Ph.D. thesis, expected April 2012) – complete all four geometries
    - Also complete modal analysis of earlier geometries

N2 properties

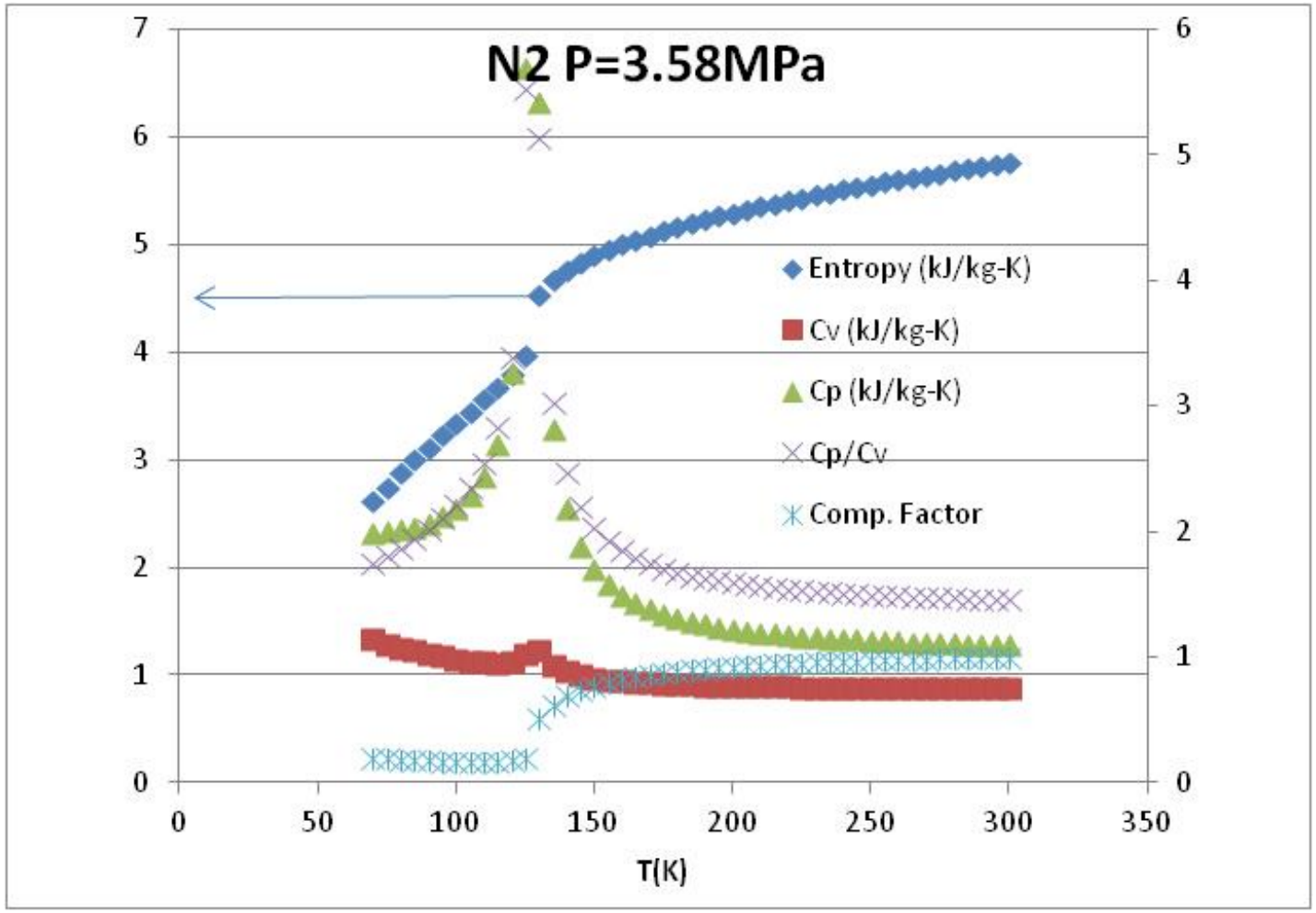

From http://webbook.nist.gov/chemistry/

N2 properties

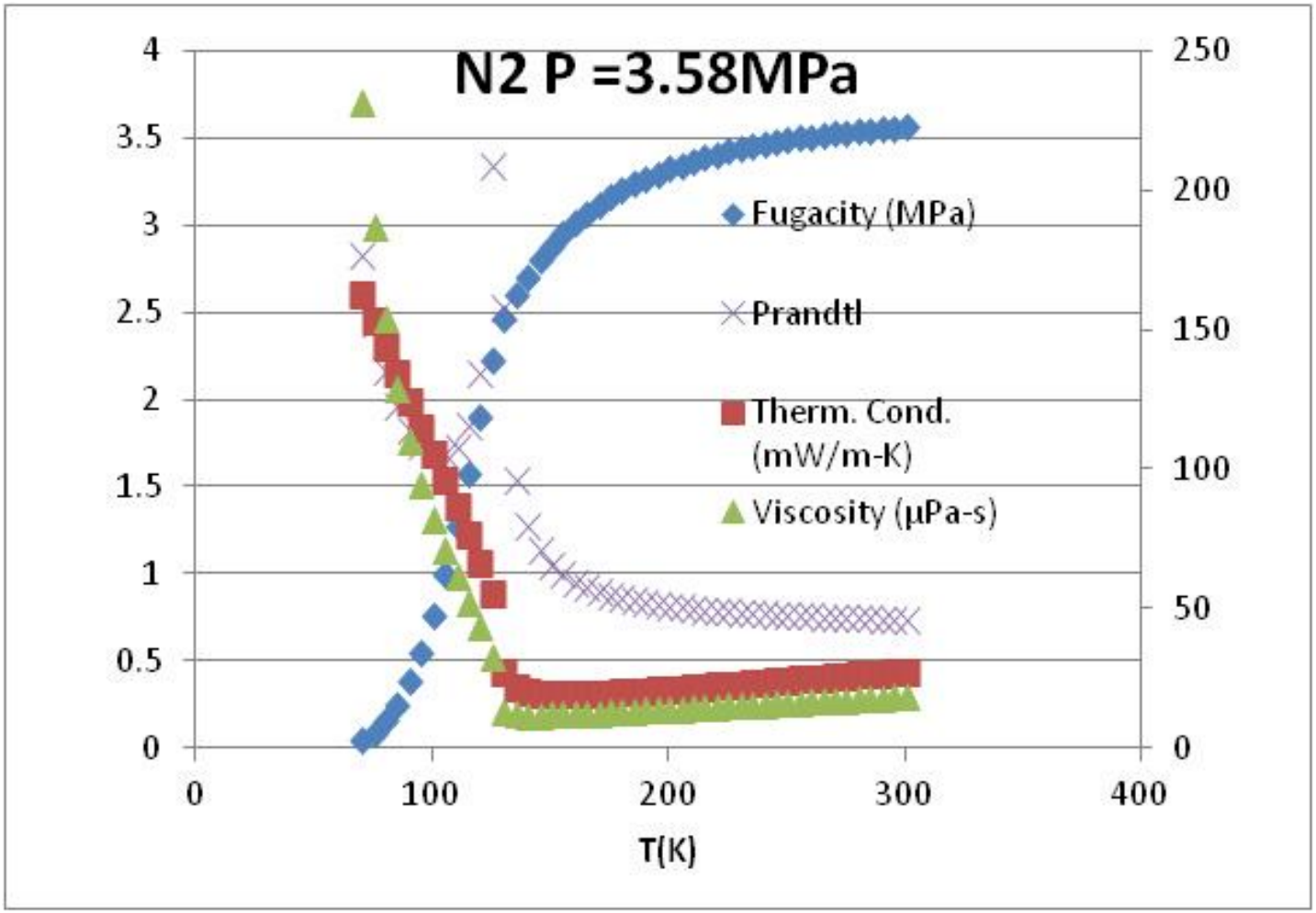

From http://webbook.nist.gov/chemistry/

N2 properties

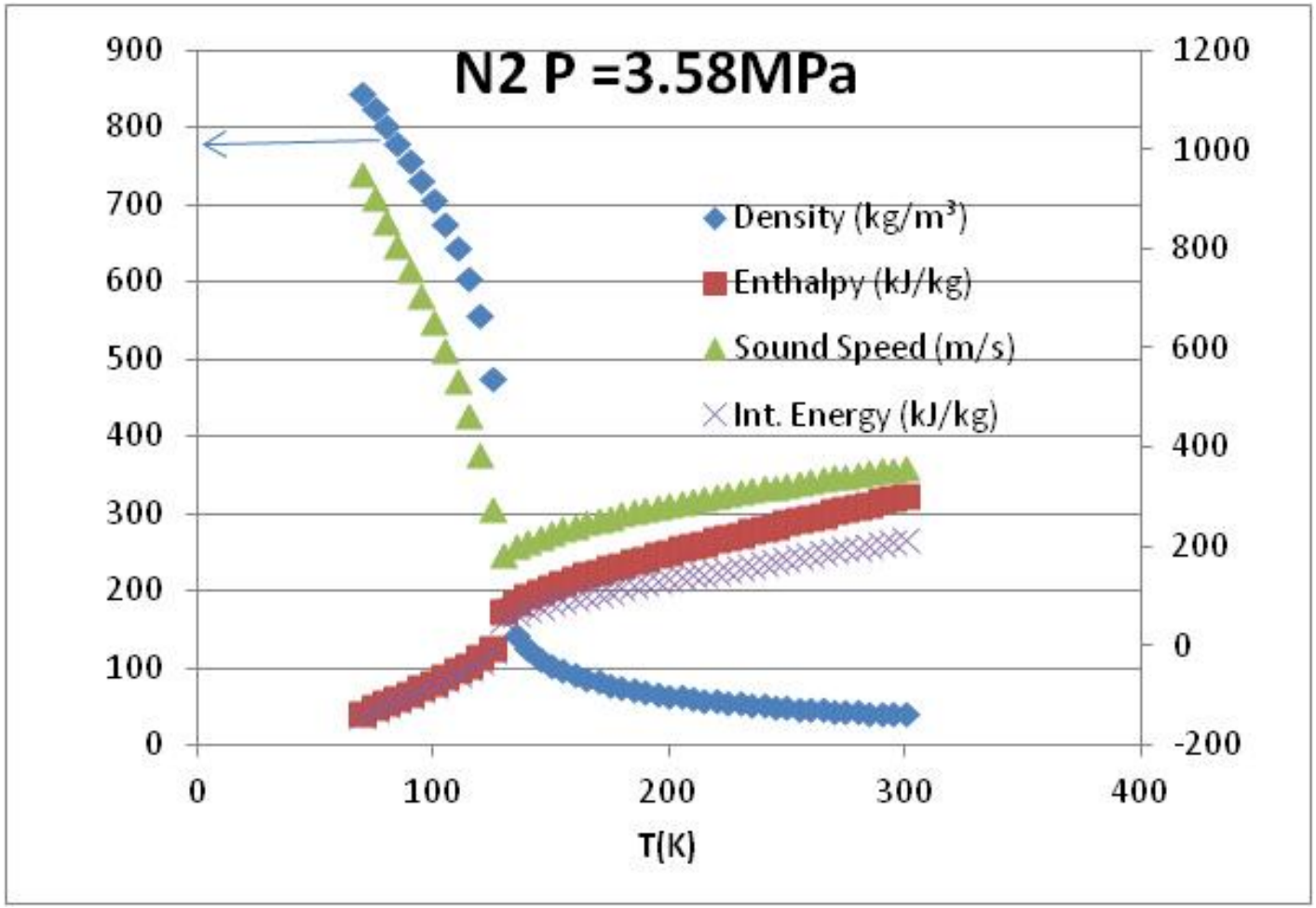

From http://webbook.nist.gov/chemistry/

N2 properties

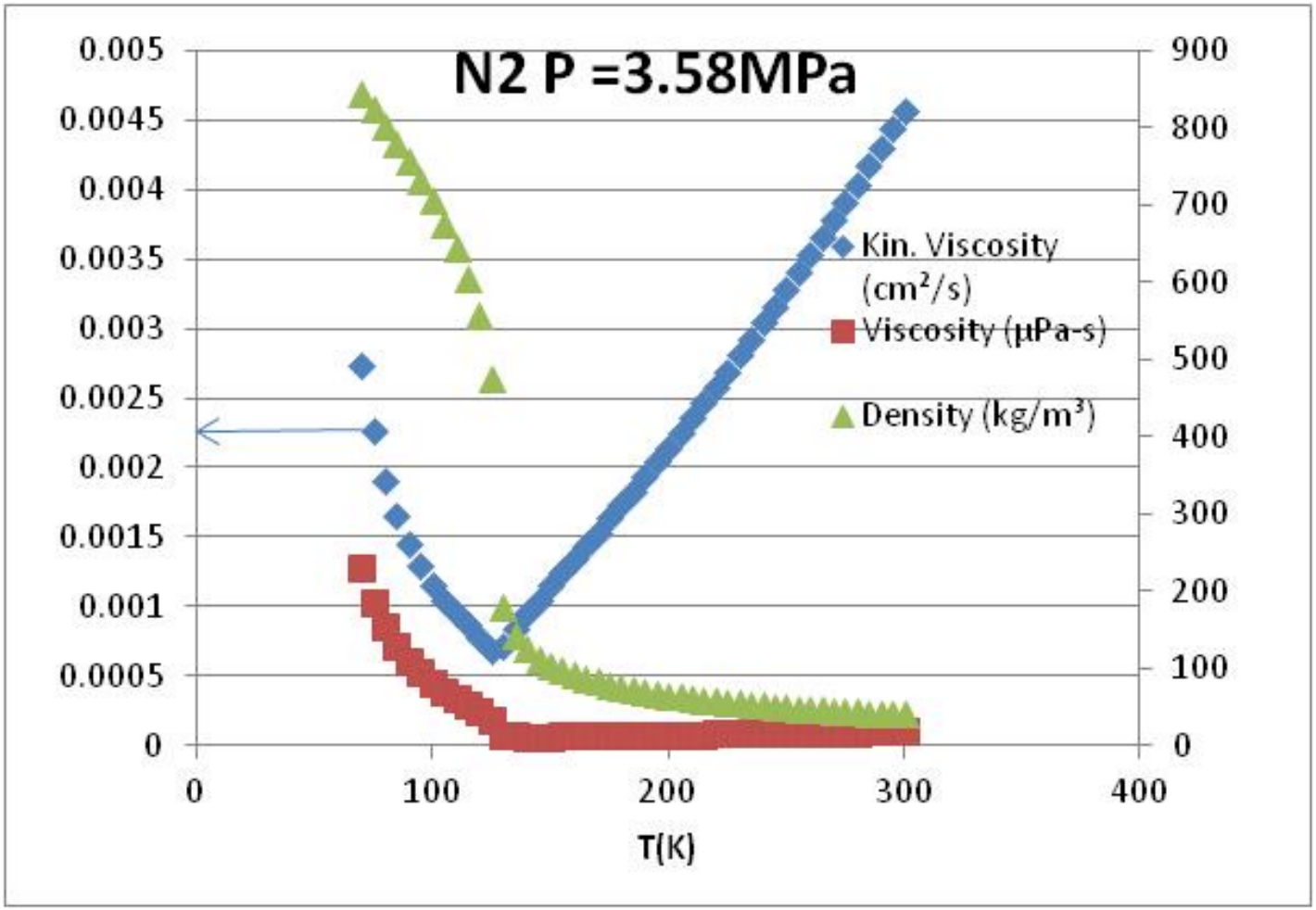

From http://webbook.nist.gov/chemistry/

Ref for Davis graph

REF	Author	Date	Fluid Inner Jet	Fluid Outer Jet	Fluid Ambient	Pressure (MPa)	T_i (K)	T_o (K)	T_∞ (K)
[44]	Forstall & Shapiro	1950	Air+ 10 %He	Air	Air	0.1*	Amb. [a]	Amb.	Amb.
[45]	Chigier & Beer	1964	Air	Air	Air	0.1*	Amb.	Amb.	Amb.
[46]	Champagne & Wygnanski	1971	Air	Air	Air	0.1	Amb.	Amb.	Amb.
[48]	Au and Ko	1987	Air	Air	Air*	0.1*	Amb.	Amb.	Amb.
[8]	Eroglu et al.	1991	Water	Air	Air	0.1*	Amb.	Amb.	Amb.
[62]	Woodward	1993	KI (aq.)	N2, He	N2, He	0.1 – 2.17	Amb.	Amb.	Amb.
[50]	Villermaux et al.[g]	1994	Water	Water	Water	0.1*	Amb.	Amb.	Amb.
[63]	Englebert et al.	1995	Water	Air	Air	0.1	293	293 – 636	293
[64]	Carreau et al.	1997	LOX	He, N2, Ar	NC[c]	0.1	82[d]	245 – 272[d]	NC
[51]	Rehab et al.[g]	1997	Water	Water	Water	0.1*	Amb.	Amb.	Amb.
[52]	Rehab et al.[g]	1998	Water	Water	Water	0.1*	Amb.	Amb.	Amb.
[53]	Villermaux [g,h]	1998	Water	Water	Water	NR	NR	NR	NR
[58]	Lasheras et al.[g]	1998	Water	Air	Air	0.1	Amb.	Amb.	Amb.
[54]	Lasheras & Hopfinger [g,i]	2000	NR	NR	NR	NR	NR	NR	NR
[60]	Favre-Marinet & Schettini	2001	Air, SF6	Air,He	Air, He	0.1	Amb.	Amb.	Amb.
[65]	Porcheron et al.	2002	LOX, Water	He, N2, Ar, Air	Air	0.1	82, 293	245 – 293	293
This work	Davis	2005	N2	N2	N2	1.4 – 4.9	108 – 133	132 – 204	197 – 249

From D.W. Davis. On the Behavior of a Shear-Coaxial Jet, Spanning Sub- to Supercritical Pressures, with and without an Externally Imposed Transverse Acoustic Field. Ph.d. dissertation, Pennsylvania State University, 2006.

Ref for Davis graph

REF	Author	Density Ratio Outer / Inner	Velocity Ratio Outer / Inner	M Outer / Inner	Re Inner ($x10^4$)	Re Outer ($x10^4$)	We
[44]	Forstall & Shapiro	1.09	0.2 - 0.75	0.04 - 0.61	NR	NR	NA
[45]	Chigier & Beer	1*	0.024 – 9.22	5.8×10^{-4} – 85.0	~10 [b]	~10 [b]	NA
[46]	Champagne & Wygnanski	1*	0 - 10	0 - 100	1.01 - 10.15	0 - 9.6	NA
[48]	Au and Ko	1*	1.25 - 6.67	1.5 - 44	NR	NR	NA
[8]	Eroglu et al.	0.001	4.5 - 131.2	0.02 - 17.2	0.15 - 0.93	2.0 - 11.6	15 - 530
[62]	Woodward	0.0006 - 0.018	0 - 30	0 - 1.7	7.86 - 18.9	NR	$12 – 3.6 \times 10^4$
[50]	Villermaux et al.[g]	1	1 - 6	1 - 36	>5000	>5000	NA
[63]	Englebert et al.	0.0008 - 0.0012	10.25 - 66.75	0.12 - 4.3	0.54 - 3.4	4.8 - 16.5	76 - 2610
[64]	Carreau et al.	NR	NR	3 - 21.5	5.32 - 8.11	NR	9.19×10^3 - 3.48×10^4
[51]	Rehab et al.[g]	1	2 - 5	4 - 25	NR[f]	NR[f]	NA
[52]	Rehab et al.[g]	1	2.2 - 5.6	4.9 - 31	1 - 10	1 - 10	NA
[53]	Villermaux [g,h]	1*	NR	NR	NR	NR	NR
[58]	Lasheras et al.[g]	0.001	NR	NR	NR	NR	NR
[54]	Lasheras & Hopfinger [g,i]	NR	NR	NR	NR	NR	NR
[60]	Favre-Marinet & Schettini	0.028 - 1	3.0 - 70	1 - 200	NR	3.2, 11.0	NA
[65]	Porcheron et al.	1.6×10^{-4} - 2.3×10^{-3}	NR	2 - 21.6	NR	NR	0 - 14000
This work	Davis	0.04 - 0.56	1.2 - 11.1	0.19 - 11.2	1.2 - 3.2	0.8 - 19	32 - ∞

From D.W. Davis. On the Behavior of a Shear-Coaxial Jet, Spanning Sub- to Supercritical Pressures, with and without an Externally Imposed Transverse Acoustic Field. Ph.d. dissertation, Pennsylvania State University, 2006.

Conclusions

- **Mixing for shear coaxial jets has other major variables other than momentum flux ratio (J)**
  - Ratio of inner jet temperatures is another important variable
  - Geometry – Area ratio and lip thickness also affect mixing
- **For LARthick**
  - Found bending mode with largest effect at velocity antinodes
  - The reduction on the dark core length was greatest for a medium J range
  - For near critical pressures, the collaboration with ECP determined relevant St for our injector configuration and was able to capture qualitative behavior of natural and excited jets
- **For SARthin**
  - Did not see bending mode for conditions studied
  - Saw vortex roll-up and puffing occurring over entire J range (0.09-21) tested –
  - PAN forcing produced symmetric flow structures regardless of *J*
  - Spectral plots showed strong response to PAN forcing at low and high *J*
- **For LARthin**
  - Sees both bending and vortex roll-up modes depending on the acoustic frequency
  - PAN forcing at low *J* produced symmetric flow structures, while at higher *J*, influence of forcing subsided
  - Spectral magnitude plots showed decreasing influence of PAN forcing with increasing *J*